General comments

We thank the reviewers very much for their diligent review of our manuscript. Their comments have been very helpful to improve it. We insert below a point-by-point response to all of them.

The most important changes to be found in this revised version of the manuscript include:

- An update of the RF calculation method, which now makes use of the CACK v1.0 dataset
- The insertion of a Figure to visually explain the methodology of the reconstruction methods, as well as the reformulation of extensive parts of the Methodology section.
- The reconstruction of the present-day albedo of trees and crops/grasses for 3 more models (GFDL-CM3, GFDL-ESM2G and GFDL-ESM2M)
- The deletion of Table S1, its values being now mentioned in the text
- The addition of a supplementary table detailing which land cover classes from the GlobCover dataset corresponds to the broad classes employed in this study
- The addition of another supplementary table listing the CMIP5 models considered in the various analyses conducted for this study, as well their respective ensemble members
- References to previous studies on the topic pointed at by the reviewers

Short Comment #1 from Ryan Bright

This is an interesting and timely study. Although its novelty aspects pertain to the surface albedo extraction methods, the authors convert albedo changes to instantaneous radiative forcings (RF) which are subsequently benchmarked to results of several climate modeling studies and to IPCC AR5 estimates. Since the RF quantification and associated benchmarking is made an integral part of the paper, I would encourage the authors to reflect on the uncertainty of their RF estimates, which are based on a very simple parameterization [i.e., Eq. (12) and Cherubini et al. (2012)] that does not account for the spatio-temporal variation in atmospheric optical properties affecting transmittance of reflected solar radiation. Bright & O'Halloran (2019), for instance, benchmarked the performance of Eq. (12) to four GCM-based kernels and found persistent positive biases (see f. ex. Fig- ures 1 & 2) and a relative RMSE of about 20% globally. Bright & O'Halloran (2019) proposed a new simplified RF parameterization (see Eq. (17)) that sub- stantially reduces RF "error" (rRMSE of about 6% globally) and made a gridded RF kernel product based on this parameterization freely available (archived here: https://doi.org/10.6073/pasta/d77b84b11be99ed4d5376d77fe0043d8). This product is based on the same underlying CERES v4 data that has been employed in this study and includes uncertainty layers.
I would therefore encourage the authors to either: a) Drop the RF quantification and benchmarking part altogether and keep the focus on the novel albedo methods and merits, or b) Provide a strong justification for using Eq. (12) in light of its uncertainty, or c) Adopt an alternate RF kernel/model that has lower uncertainty.

Bright & O'Halloran 2019: https://www.geosci-model-dev.net/12/3975/2019/gmd-12-3975-2019.html

Thank you very much for the comment and the great suggestion. We have decided to use the CERES-based albedo change albedo kernel (CACK) from Bright and O'Halloran (2019) for the Radiative Forcing calculations. As a result, the values of global RF associated with

historical conversions between trees and crops/grasses are systematically less negative by ~20-30% for each of the CMIP5 models considered in Section 5 (see the revised versions of what are now Figures 12 and 13).

Anonymous Referee #1

Overall opinion: Lejeune et al. have devised an interesting and innovative method for extracting the albedo of forested and crop/grass land cover types from model simulations and the combination with the space-for-time approach to estimating the effect of land cover change is quite promising. I feel the science is of good quality and the results are useful.

Thanks to the reviewer for the useful and overall positive comments.

Some questions: I agree with the already posted comment that the RF estimates are based on a parameterization that may contribute its own biases and that the strength of the paper is in the novel albedo methods. I leave it up to the authors whether to address this in the discussion or to change the RF parameterization.

As specified in the response to Ryan Bright's comment, we have decided to follow his suggestion to use the CERES-based albedo change albedo kernel (CACK) from Bright and O'Halloran (2019) for the Radiative Forcing calculations. As a result, the values of global RF associated with historical conversions between trees and crops/grasses are systematically less negative by ~20-30% for each of the CMIP5 models considered in Section 5 (see the revised versions of what are now Figures 12 and 13).

Differences in soil type or texture can affect the albedo of vegetated surfaces and that this would add noise, if not bias to the 'space for time' method.

Surface albedo is indeed influenced by both the vegetation canopy and the soil, and this is the case in both satellite-derived observational products and climate models. It is true that both the vegetation canopy and the soil can exhibit variations in solar reflectance even for a same land cover, e.g. due to variations in Leaf Area Index or in soil texture. If such variations occur within a 'big box' of 5X5 grid cells, this can indeed introduce noise to the reconstruction methodology, and thus explain a substantial part of the RMSE of the reconstruction methodology discussed in Section 3.

Some brief discussion of the quality, accuracy or uncertainty in the datasets employed (e.g. ESA-CCI) would be helpful.

In the revised manuscript, we have added brief discussions of the quality of the employed observational datasets. The GlobAlbedo and MODIS MCD43C3 albedo products are considered to be of very good quality overall and show good agreement (global R^2 of 0.85). Some problems associated with snow detection were identified in GlobAlbedo but the resulting artifacts are most significant at very high latitudes (>70°), which are of lesser interest for our study (Muller et al, 2013). Imprecisions in land cover datasets such as GlobCover and ESA-CCI may especially arise via misclassification between land cover types within the broad trees or crops/grasses classes (e.g., between two types of trees) or the difficulty to properly identify medium-sized or mixed-type vegetation (i.e., shrub or savanna-

like). In contrast, because these products are best at distinguishing very distinct land cover types such as trees and crops/grasses, the satellite-derived albedo values of these two broad classes (retrieved following the methodology presented in Section 2.1.1) as well as their differences (obtained from the D18 data) are characterised by relatively low uncertainties.

I am curious as to why CRUNCEP V4 was chosen for offline simulations when newer versions and reportedly improved products such as CRUJRA and GSWP3 are available.

At the time the CLM4.5 simulation was conducted, CRUNCEP V4 was the recommended forcing data set (Chapter 26 in Oleson et al., 2013). Indeed, CLM offline simulations forced by GSWP3 represent surface albedo better than simulations forced by CRUNCEP (http://www.cesm.ucar.edu/models/cesm2/land/). However, the main purpose of this simulation is to demonstrate that the reconstruction method retrieves similar albedo alterations due to land-cover changes as the subgrid method. Therefore, the performance of this particular simulation is no major concern, as long as the simulated albedo is realistic to a sufficient extent.

Specific minor details:

Line 23: Doesn't constraining something usually reduce its range?

"Constraining" the global RF estimates by using the albedo changes due to conversions between trees and crops/grasses from satellite data instead of the individual CMIP5 models indeed leads to a somewhat unexpected increase in the model range. This result occurs because of two models which exhibit unrealistic historical conversion rates from trees to crops/grasses, which we therefore decided to discard for the final estimation of the RF from historical land-cover changes.

Line 26-28: Awk-ward sentence Multiple locations: "associated to" should be "associated with" Multiple locations: "inferior to" should be "less than" and "superior to" should be "greater than"

Line 300: Change "the local albedo difference between albedo and crops/grasses" to "the local albedo difference between forest and crops/grasses"

We have taken these remarks concerning the language into account when revising the manuscript and reformulated the relevant sentences.

References:

Muller, J.-P. et al. (2013) GlobAlbedo Final Product Validation Report.

Oleson, K. W. et al. (2013) 'NCAR/TN-503+STR NCAR Technical Note Technical Description of version 4.5 of the Community Land Model (CLM) Coordinating Lead Authors'. Available at: http://library.ucar.edu/research/publish-technote (Accessed: 31 December 2019).

Anonymous Referee #2

Summary: The authors attempt to train statistical models to extract the albedo of specific land cover classes in CMIP5 models, with the intent to then calculate the albedo change, and associated radiative forcing (RF), due to deforestation over the historical period. The paper is concise, and reasonably well written, although I found the description of the reconstruction methods to be somewhat unclear. The goals of the research are novel and highly relevant for the land surface and climate modelling communities, and I believe that this work will be suitable for publication once several important concerns are addressed.

We thank the reviewer for taking the time to go through the manuscript and submitting detailed comments. We are providing answers to these below, by referring to the in- dividual comments through mentions of the same line numbers given by the reviewer. We also attach a point-by-point response including the reviewer's comments, which may facilitate the second round of reviews.

Major comments:

-L158: I found the description of the reconstruction method hard to follow, perhaps because several different types of regression models were being applied simultaneously, and perhaps also because non-technical terms like "big box" were introduced. I think a simple diagram, showing the big box and the target (central) cell, and some of the most important quantities involved in the regression models, would be helpful to better explain the methods.

We have extensively worked on improving the methodology description. Including a figure was indeed a good idea to facilitate its understanding by the reader, and we have followed this piece of advice from the reviewer. The new Figure 1 should clarify non-common technical terms like "big box", the used reconstruction methods and some methodological steps we apply to increase their reliability.

-L235: The authors use an empirical parametrization to relate changes in surface albedo from deforestation to RF at Top of Atmosphere. While this approach is simple and straightforward, I wonder why the authors could not apply a surface albedo radiative kernel instead, as it removes the assumption of temporal and spatial homogeneity in atmospheric transmittance. Given that both surface and TOA clear sky kernels are publicly available, this minor methodological revision would be efficient and most useful. At the very least, the authors could validate their empirical parametrization against a radiative kernel with sample data. The authors are clear to cite the use of such a parametrization in other work. However, given that the the paper attempts to provide a precise, constrained RF estimate from historical deforestation, removing any limitation associated with such a result would provide a significant improvement to the manuscript.

All reviewers have suggested to use a different kernel to convert the reconstructed historical albedo changes due to conversions between trees and crops/grasses into RF estimates. Following Ryan Bright's comment, we have decided to use the version 1.0 of the CERES-based albedo change kernel (CACK) from Bright and O'Halloran (2019) for the Radiative Forcing calculations. This kernel is based on a novel, simplified parameterisation of shortwave radiative transfer and driven with downwelling shortwave radiation values at the surface and the top of the atmosphere obtained from the Clouds and the Earth's Radiant Energy System (CERES) Energy Balance and Filled (EBAF) 1°-resolution products. CACK

was evaluated by Bright and O'Halloran (2019): While being more easily understandable and easier to apply than kernels derived from climate models, it is able to mimick them more faithfully than five previously employed analytical, semi-empirical and empirical kernels.

-L284: In Figure 2, the authors show the reconstructed albedo of crops/grasses over northern Eurasia is essentially the albedo of snow (>0.8). Therefore, I take issue with the authors describing their reconstruction as the "extraction of the correct albedo values of specific land cover". This statement is true for the July reconstruction, but the underlying albedo of the vegetation in January is not 0.8, it is most likely very similar to the July value (~0.2). Therefore, to avoid any potential for confusing the reader, I would like the authors to describe clearly what is being extracted, which is the surface albedo of grid cells with different *underlying* land cover classes".

-L284: The reviewer is right that the surface albedo in both observational data and climate models is influenced by both the vegetation canopy and the soil reflectance. We have now clarified this at the beginning of Section 2.1.1. For the sake of simplicity, we however use the formulation "albedo of a specific land cover class" when referring to this mixed contribution of the soil and canopy to the surface albedo. This has also made clear in Section 2.1.1.

I note that the same issue also appears to be present in the reconstructed estimate of January albedos in Figures 6 and 8. Therefore, is it possible using this method to be certain that the albedo change due to LCC (e.g. Figure 10), and associated RF (Figure 11), is properly separated from the albedo change due to changes in snow accumulation and melt over the historical period?

We would like to stress that the present-day albedo of trees and crops/grasses is only reconstructed following the method described in Section 2.3.1 in order to be evaluated against satellite-derived data, as discussed in Section 4 and illustrated in Figures 6-11. In contrast, the historical albedo changes associated with transitions between trees and crops/grasses between the pre-industrial and 1981-2000 periods are reconstructed following the method described in Section 2.3.2, so that the associated global RF can be derived and discussed in Section 5 (based on Figures 12 and 13) in light of the model biases identified using the first reconstruction method. We acknowledge that this may have been ambiguous in the submitted manuscript, and intended to make it clearer in the revised version.

That being said, changes in surface albedo over vegetated surfaces between the pre-industrial and present-day periods are mainly influenced by changes in albedo of the vegetation canopy, in the fraction of ground (soil or snow) that is shed from sunlight by the vegetation canopy, and in the albedo of the ground. The first two contributions are mostly influenced by LCC and in particular transitions between trees and crops/grasses. They are therefore included in the term γ_1 of Equation (7). The latter contribution is mostly influenced by other climate forcings such as greenhouse gases, whose influence has a larger spatial extent which is thus assumed to be con-stant across a big box and included in the term γ_0. For the models for which factorial experiments (with LCC only or with all forcings except LCC) are available, we were able to directly extract the simulated change in surface albedo due to LCC. The similarities between these direct estimates and the results from the reconstructed method (compare the columns on the left and right sides of Figures S6, S7, S11 and S13) confirm the ability to properly separate surface albedo changes due to LCC from those due to changes in snow accumulation and melt. Some differences are found for the GFDL-ESM2 model but both estimates remain compatible given the uncertainty ranges of each method (see Figure S21).

-L311: In Section 3 the authors perform a validation of the reconstruction, and find errors in the reconstructed albedo in the range 10-40%. They conclude at the end of the Section that this method is appropriate to apply to CMIP5 models. But I would have appreciated a little more rigour in this part of the analysis; for example, the authors should define a priori what an acceptable tolerance of error would be. In other words, define what constitutes a "useful" estimate of albedo, which would provide the reader with a stronger basis for interpreting whether 10-40% error is acceptable. Since the focus later is on RF, perhaps one way to define "useful" is in terms of the perturbation that the uncertainty in albedo estimate passes on to the RF calculation, in energy units?

The present-day albedo of trees and crops/grasses that is reconstructed in the CMIP5 simulations using the methodology described in Section 2.3.1 is not used later on in the RF calculations, but simply to be evaluated against reference satellite-derived data. This evaluation effort reveals that, in some of the analysed CMIP5 models, the reconstructed albedo changes associated with transitions from trees to crops/grasses can differ from the reference values from Duveiller et al. (2018) by ~0.05 (respectively, ~0.4) over snow-free (respectively, snow-covered) areas (see Figures 10 and 11). These differences being substantially higher than the RMSE of the reconstruction (which amounts to ~0.02 over snow-free and ~0.05 over snow-covered areas, see Figures 4 and 5), we argue that the reconstruction method is useful to identify biases of CMIP5 models. We have included a paragraph justifying this thinking more extensively at the end of Section 3.2.

-L321: The authors find considerable intermodel differences in albedo biases, but I couldn't see any discussion linking the different biases to the underlying satellite-derived vegetation datasets used by each modelling group to calibrate their land models. In the case of CanESM2, it's the GLC2000, whereas for models using CLM it is MODIS. Could the authors investigate whether this difference is a contributing factor to the biases? And if so, perhaps the authors could make recommendations to the community as to which datasets produce the lowest biases?

Because our analysis focuses on the potential albedo change resulting from a land cover conversion between trees and crops/grasses rather than the mean surface albedo of each model grid cell, differences in the vegetation distributions of individual models should play a limited role in the biases identified in Figures 6-11. It is however true that if a model has a too low proportion of trees in a given region, for example, it can hinder the retrieval of the albedo of trees in this same region and therefore limits the scope of our analysis. However, we expect these effects to be of secondary importance.

L335: The discussion of biases in forested albedo when snow is present reminded me of the work by Thackeray et al. (2015, doi=10.1002/2015JD023325), and Wang et al. (2016, doi=10.1002/2015JD023824). I think that citations and connections to these previous studies would be helpful here to explain your results. In addition, Thackeray (2014, doi=10.1002/2014JD021858) shows that the parameterization of canopy albedo in CLM4 was overly sensitive to temperature, resulting in a seasonal cycle that differed significantly from observations.

The papers by Thackeray et al. (2014, doi=10.1002/2014JD021858 and 2015, doi=10.1002/2015JD023325), as well as Wang et al. (2016, doi=10.1002/2015JD023824) brought to our attention by the reviewer are indeed very relevant for the interpretation of our results. They point at model deficiencies which relate to some of the biases identified in our study, such as the too high albedo of trees in snow-covered areas in the MIROC5 and GFDL-ESM2M models. We have included references to these papers in the Results section (4.1.1), as well as in the Discussion and Conclusions section (6).

Minor comments:
-L82 and throughout: I suggest replacing all occurrences of "associated to" –> "associated with".
-L300: "albedo difference between albedo and crops/grasses" –> should this say "be- tween *trees* and crops/grasses"?
-L305: "remain similar" to what?
-L309: I suggest here citing some previous work on computing the "snow-masking effect of forests", for example by Essery (2013).

We have taken these minor comments into account when preparing the revised manuscript.

References:

Bright, R. M. and O'halloran, T. L. (2019) 'Developing a monthly radiative kernel for surface albedo change from satellite climatologies of Earth's shortwave radiation budget: CACK v1.0', *Geosci. Model Dev*, 12, pp. 3975–3990. doi: 10.5194/gmd-12-3975-2019.

Duveiller, G., Hooker, J. and Cescatti, A. (2018a) 'A dataset mapping the potential biophysical effects of vegetation cover change', *Scientific Data*. Nature Publishing Groups, 5. doi: 10.1038/sdata.2018.14.

Anonymous Referee #3

This paper presents an approach to diagnosing CMIP5 model outputs with regard to the albedo changes and hence resultant radiative forcing from land cover change from trees to crops/grasses. It borrows the ideas from the analysis of observational data, that is, space for time to reconstruct albedo values of trees and crops/grasses and their differences via an unmixing technique based on linear regression over grid cells within local spatial windows. It compares results among CMIP5 models and between these models and observational data. The evaluation of the reconstruction approach using a model CLM also helps us understand the effectiveness of this approach that has been used to analyze observational data. The study uses both observational and modeling data that varies in terms of native spatial resolutions, temporal resolutions, and temporal coverages. This diversity in data strengths the investigation but also requires more efforts to achieve a clear and lucid description of methodology and results. I found the description of the methodology and the presentation of the results need some particular improvements. I admit that my knowledge is more on the observational side of studies on land cover and biophysical effects. Some of my questions may have common answers within the hard-core modelling community. Nonetheless, I believe addressing these issues would help the comprehension of the study by a wider audience.

Many thanks to the reviewer for taking the time to go through the manuscript and submitting such detailed comments. This is very helpful to improve the manuscript.
We are providing answers to the reviewer's comments below.

First, Section 2.3.1 needs some clarification in text. I have several questions concerning the understanding of the described method. See detailed comments below. In particular, the line 191-192 states a post-reconstruction estimates of albedo changes by calculating the differences in albedo between trees and crops/grasses. Then the section 2.3.2 looks like a

direct estimate of albedo changes from deforestation rate. So, what is the distinction between post-reconstruction estimates and the direct estimates in Section 2.3.2? And which estimates of albedo changes do you present in the results, e.g. Fig. 3, 4, and 9 to 13, and Table 1?

We indeed introduce two different reconstruction methods in the manuscript. We aim at clarifying the methodology section in a revised version of the manuscript, and especially at explaining better what these two methods intend to do and how. We also hope that the newly included Figure 1 will provide visual help in that respect. In this study we reconstruct two different quantities in CMIP5 models: 1) the simulated present-day albedo of trees and crops/grasses, to evaluate the albedo change arising from a potential transition between these two classes against observational data, and 2) the historical surface albedo changes associated with transitions between trees and crops/grasses, followed by an assessment of their consequence in terms of Radiative Forcing. Based on Figures 2-5, Section 3 focuses on the evaluation of the ability of the first employed reconstruction method to extract the first quantity (simulated present-day albedo of trees and crops/grasses) in CMIP5 all-forcings simulations. In Section 4, based on Figures 6-11 we evaluate the albedo change arising from a potential transition between trees and crops/grasses in CMIP5 models against observational data. This quantity has been extracted using the first reconstruction method, which has previously been evaluated in Section 3. In Section 5, based on Figures 12-14 we discuss the historical surface albedo changes associated with transitions between trees and crops/grasses between the pre-industrial and 1981-2000 periods, and which have been reconstructed in CMIP5 models using the second reconstruction method.

Second, as you use observational and modeling data of different temporal spans/coverages, please specify the year/temporal periods or the temporal coverages for all the figures and tables. For example, Fig 1 & 2, which year/temporal periods are you presenting? In particular for albedo changes, between which year/temporal periods are the presented difference, e.g., Fig. 3 & 4. Almost all the figure/table captions need such clarification. Also, better clarify the spatial resolution of your results. I haven't found explicit statement on the spatial resolution of your reconstructed albedo per land cover class or reconstructed albedo changes per land cover change from trees to crops/grasses. Line 158 says "big boxes of a size of 5 times 5 grid cells", and the grid cells of CMIP5 model outputs you are using have a size of 2 deg (line 90). Does this mean your reconstructed albedo values and albedo changes have a resolution of 10 deg?!

Following the reviewer's comment, we have now specified the relevant temporal periods in the legends of the Figures. Moreover, the revised methodology section as well as the new Figure 1 should make clearer that within one big box, we reconstruct the albedo values (or albedo changes) for the grid cell in the center of the big box, i.e. the reconstructed albedo values and albedo changes have the original model resolution (about 2°).

Third, about the radiative forcing from albedo changes. Here you are estimating and showing spatially-explicit RF. I'm not convinced that a single value for k (line 242-243) is enough to account for different solar angles at different latitudes. In Lenton and Vaughan (2009), they were looking into the global effect of geoengineering and a single value of k based on annual global mean transmittance was justified. But I'm convinced it is justified here. Also do you calculate RF from albedo changes month by month? Your presented results seems annual average of RF (fig. 11, 12). Then how do you average monthly changes since your reconstructed albedo changes clearly show monthly differences (fig. 3, 4, 9, 10)

All reviewers have suggested to use a different kernel to convert the reconstructed historical albedo changes due to conversions between trees and crops/grasses into RF estimates.

Following Ryan Bright's comment, we have decided to use the version 1.0 of the CERES-based albedo change kernel (CACK) from Bright and O'Halloran (2019) for the Radiative Forcing calculations. This kernel is based on a novel, simplified parameterisation of shortwave radiative transfer and driven with downwelling shortwave radiation values at the surface and the top of the atmosphere obtained from the Clouds and the Earth's Radiant Energy System (CERES) Energy Balance and Filled (EBAF) 1°-resolution products. CACK was evaluated by Bright and O'Halloran (2019): While being more easily understandable and easier to apply than kernels derived from climate models, it is able to mimick them more faithfully than five previously employed analytical, semi-empirical and empirical kernels. CACK provides a monthly climatology, thus since we reconstruct the albedo changes associated with historical conversions between trees and crops/grasses for each month (see Section 2.3.2), we can also compute an annual mean associated RF by averaging the contributions from each month (Equation 10).

Detailed comments,

1. Line 85-90, Please, even if just in supplementary materials, provide an explicit translation from GlobCover's land cover legend into your trees and crops/grasses for traceability.

As asked by the reviewer, we have included an explicit translation from GlobCover's land cover classification into the two broad classes that we used (trees and crops/grasses) in a new Table S1, and added a reference to this Table in Section 2.1.1.

2. Line 89, black sky albedo at what solar angle?

We understand that the GlobAlbedo product makes use of an optimal estimation approach including angular integrals and a gap-filling technique based on the MODIS surface anisotropy dataset in order to integrate data derived from the Advanced Along-Track Scanning Radiometer (AATSR), SPOT4-VEGETATION, SPOT5-VEGETATION2, and MERIS instruments, which exhibit different spectral and angular sampling. We have included this information in Section 2.1.1.

3. Section 2.1.2, specify the spatial resolution of D18 data in degrees for easier reading and easier comparison between presented datasets.

The resolution of the dataset from Duveiller et al. (1°) was missing and has now been specified in Section 2.1.2.

4. Line 131, Each grid cell in D18 dataset refers to a specific land cover change, i.e. a pair of land cover classes. What do you mean here by grouping land cover fractions in CMIP5 outputs within one land cover class? Furthermore, D18 provides albedo changes for 45 land cover transitions. How come the consistency with D18 is the reason for focusing just on transition between trees and crops/grasses?

As specified in Section 2.1.2, we have used the version of the D18 dataset that provides albedo changes for only six land cover transitions between four broad land cover classes (forests, shrubs, crops/grasses and savannas). This classification scheme is referred to as IGBPgen in the paper describing the dataset. Consistently with this scheme, when represented in the CMIP5 models we have considered grasses, crops and pasture as belonging to one single class: crops/grasses.

5. Line 165, “inferior to” and “superior to”. . . . maybe just simply say "less than".... ? simple words like "larger than" is enough and better for reading? There are more such cases in the rest of the text to be fixed.

We have now revised these formulations.

6. Line 184 – 185, What does it mean by "land cover classes are represented" in a grid cell? lcf is larger than zero? If fewer than two grid cells have lcf > 0 for a class, then this class will not be considered in the regression at all. The Eq (2) will have one fewer term on the right side? But will that one grid cell with lcf > 0 (if there is one) for this class be used in such a regression that does not include this class? If so, isn’t this inappropriate? If not, please clarify here.

The sentence originally containing “land cover classes are represented in a grid cell” has been reformulated as such: “Therefore, each predictor (lcf_{tr}, lcf_{sh}, lcf_{cg} is only included in the regression (i.e., its corresponding term is included in Equation 1 or 2) if its value is greater than 0 in at least two snow-free (if *i* is snow-free) or snow-covered grid cells (if *i* is snow-covered).” If for example lcf_{sh} is not included in a regression, that one grid cell with $lcf_{sh} > 0$ (if there is one) may still be considered in the regression if over that grid cell $lcf_{tr} + lcf_{cg} > 90\%$. This would effectively mean that lcf_{sh} is less than 10%, therefore that the albedo of shrubs only accounts for a small portion of the mean surface albedo over that grid cell.

7. Line 186–187,15 is more than half of 25 grid cells in a big box. So in each big box, you can only estimate albedo for either snow-covered land cover classes or snow-free land cover classes. But NOT for both snow-covered and snow-free?

The referee is correct that if a grid cell is snow-free (respectively, snow-covered) in a given month, we only estimate albedo for snow-free (respectively, snow-covered) conditions. We have reformulated parts of Section 2.3.1 to clarify this point, and the new Figure 1 should also help in that respect.

8. Line 187, “where the sum of all the included predictors exceeds 90%.”, Please clarify this sentence. Do you mean that at least 90% areal fraction of a big box, that is 0.9*25cells=22.5 cells-equivalent area, is needed for the sum of all the lcf over the included snow-covered OR snow-free grid cells? Or 90% is per EACH grid cell? This sentence reads like the former/first explanation.

We have reformulated the sentence originally present line 187 as such: “Moreover, the regressions are only conducted in the big boxes that have at least 15 grid cells (either snow-

free or snow-covered) in which the sum of all the included predictors exceeds 90%." We hope that the inclusion of the new Figure 1 will also help to make this methodological point clearer.

9. Section 2.3.2, Eq. (9) and (10), Confusing symbols and texts here. What is difference between the meanings of the $\delta\alpha_{tr\rightarrow cg}$ in Eq. (9) and the $\delta\alpha_{tr\rightarrow cg}$ (i) in Eq. (10)? The $\delta\alpha_{tr\rightarrow cg}$ in Eq. (9) is albedo change as a results of transition from trees to crops/grasses. To me, this means the same as albedo changes due to deforestation that is defined by the $lcc_{tr\rightarrow cg}$, transition rate from trees to crops/grasses. If $\delta\alpha_{tr\rightarrow cg}$ in Eq (9) is a known quantity since you need it for the regression and it means the albedo change due to deforestation, what is the physical rational of the Eq (9)? And what is the point of using regression to achieve the estimate by Eq. (10)? And how did you get the value of $\delta\alpha_{tr\rightarrow cg}$ on the left side of the Eq. (9)? Is it from the methods given in Section 2.3.1 line 191-192? Please clarify.

There was indeed a mistake, there should have been no subscript on the term on the left side of Eq. 9 (now 7). This has now been corrected.

10. Line 218, "a jackknife resampling is conducted: Alternatively, and as", some typo here? esp. about the weird punctuation marks?

The description of the jackknife resampling at the end of Section 2.3.2 has been reformulated.

11. Line 248, the $\delta\alpha_{tr\rightarrow cg}$ is estimated per month. Do you also estimate RF per month?

We indeed estimate the instantaneous RF resulting from historical conversions from trees to crops/grasses for each month, then compute the annual mean value. We hope that the revised methodology description and in particular the newly introduced Equation 10 clarify this.

12. Line 250-251, it reads very unclear even considering the preceding texts and the context. Please elaborate on this.

In an attempt to clarify this Section 2.4, we now use different notations for the present-day potential surface albedo change associated with a transition from trees to crops/grasses ($\delta\alpha_{tr\rightarrow cg}$, reconstructed using the method described in Section 2.3.1) and the historical surface albedo changes due to conversions between trees and crops/grasses between the pre-industrial and 1981-2000 periods ($\Delta\alpha_{tr\rightarrow cg}$, reconstructed using the method described in Section 2.3.2). Newly introduced Equations (11) and (12) should also help clarify this.

13. Section 2.5, no information about how you estimated albedo changes of land cover change from trees to crops/grasses in this subgrid experiment. But your results presented such subgrid estimates of albedo changes (figure 3&4, table 1).

We have tried to formulate a clearer explanation of how the subgrid estimates of the present-day albedo of trees and crops/grasses are extracted from the CLM4.5 simulations.

Especially, the following sentences should help to understand this point: “Surface albedo values were output for each tile in these simulations, enabling to extract a subgrid albedo value for each land cover class (trees or crops/grasses, similarly as in Malyshev et al., 2015; Meier et al., 2018). For each grid cell and each month, the albedo values for these two land cover classes are computed as the area weighted mean albedo across each PFT pertaining to the respective class over the analysis period. This reference value, later referred to as “subgrid” estimate, can then be compared to the reconstructed albedo values.”

Malyshev, S. et al. (2015) ‘Contrasting Local versus Regional Effects of Land-Use-Change-Induced Heterogeneity on Histori- cal Climate: Analysis with the GFDL Earth System Model’, Journal of Climate, 28, pp. 5448–5469. doi: 10.1175/JCLI-D-14-00586.1.

Meier, R. et al. (2018) ‘Evaluating and improving the Community Land Model’s sensitivity to land cover’, Biogeosciences, 15, pp. 4731–4757. doi: 10.5194/bg-15-4731-2018.

14. Line 263, what do you mean by "pixel" here? A grid cell in the CLM simulation? If so, be consistent in the terminology.

„Pixel“ has been changed to „grid cell“ in Section 2.5 to ensure consistency across the manuscript and more clarity for the reader.

15. Line 263 – 265, Do you differentiate snow-covered and snow-free fractions of a grid cell when you calculate albedo values for trees or crops/grasses in this area-weighted average? If so, can you provide some explanation here?

We don’t differentiate between snow-covered and snow-free grid cells when looking at the subgrid albedo values for trees and crops/grasses, but extract the subgrid albedo values for any snow cover fraction.

16. Section 3.2, Which estimate of albedo changes are you presenting here, the estimate by Section 2.3.1, line 191-192, or the estimate by Section 2.3.2?

In Section 3 we focus on the evaluation of the ability of the first employed reconstruction method (presented in Section 2.3.1) to extract the simulated present-day albedo of trees and crops/grasses in CMIP5 all-forcings simulations.

17. Line 464, what information in “for which this information is available”? This last part reads redundant and only adds confusion to this sentence.

The sentence has been reformulated: “We then demonstrated that the methodology gives estimates of the albedo of trees and crops/grasses that are close to the reference values provided at the sub-gridcell level in simulations for which these values available.”

18. Fig. 1 caption, what’s the absolute difference here? You mean albedo values?

As hinted by the Referee's comment, there was a mistake in the legend of Figure 1 and "absolute differences" should read "albedo values". This has now been corrected.

19. Almost all the figures of maps, good to have the maps here for spatial comparison. But it is only qualitative. Can you present a scatter plot over common grid cells between subgrid estimates and reconstructed estimates?

In Figures 2-5, we have now included scatter plots over common grid cells between subgrid and reconstructed estimates of albedo values (Figures 2&3) or albedo differences between trees and crops/grasses (Figures 4&5) in the CLM4.5 simulations. These plots support the discussion in Section 3 of the performance of the first reconstruction method (described in Section 2.3.1).

20. Fig. 10 v.s. Fig. 11, why the different sets of models for albedo changes and RF?

20. The first reconstruction method (described in Section 2.3.1) requires information on the snow cover fraction (snc), which therefore limits the set of CMIP5 models that can be analysed compared to the second one (described in Section 2.3.2). Moreover, for the RF analysis we consider only the CMIP5 models for which at least two ensemble members are available in an attempt to limit the uncertainties of the method. These criteria explain why the Figures 6-11 and 12-14 are based on two different sets of models.

21. Fig. 11, why not present a model mean as fig. 12?

21. We had originally chosen not to present a model mean for Figure 11 (now Figure 12) because it would have required regridding the results from the individual models to a common grid, but this is now done anyways to make the model results fit with the resolution of the CACK data. We have therefore also added a model mean for the unconstrained RF in the revised manuscript.

Biases in the albedo sensitivity to deforestation in CMIP5 models and their impacts on the associated historical radiative forcing

Quentin Lejeune[1,2], Edouard L. Davin[2], Grégory Duveiller[3], Bas Crezee[2], Ronny Meier[2], Alessandro Cescatti[3], Sonia I. Seneviratne[2]

[1]Climate Analytics, Berlin, 10969, Germany
[2]Institute for Atmospheric and Climate Science, ETH Zurich, Zurich, 8092, Switzerland
[3]European Commission Joint Research Centre, Ispra (VA), 21027, Italy

Correspondence to: Quentin Lejeune (quentin.lejeune@climateanalytics.org)

Abstract. Climate model biases in the representation of albedo variations between land cover types contribute to uncertainties on the climate impact of land cover changes since pre-industrial times, and especially on the associated radiative forcing. The recent publications of new observation-based datasets offer opportunities to investigate these biases and their impact on historical albedo changes in simulations from the fifth phase of the Coupled Model Intercomparison Project (CMIP5). Conducting such an assessment is however complicated by the non-availability of albedo values for specific land cover types, as well as the limited number of simulations isolating the land use forcing in CMIP. In this study, we demonstrate the suitability of a new methodology to extract the albedo of trees and crops/grasses in standard climate model simulations. We then apply it to historical runs from 16 CMIP5 models and compare the obtained results to satellite-derived reference data. This allows us to identify substantial biases in the representation of the albedo of trees, crops/grasses, and the surface albedo change due to the transition between these two land cover types in the analysed models. Additionally, we reconstruct the local surface albedo changes induced by historical conversions between trees and crops/grasses for 15 CMIP5 models. This allows us to derive estimates of the albedo-induced radiative forcing from land cover changes since pre-industrial times. We find a multi-model range from 0 to -0.17 W/m^2, with a mean value of -0.05 W/m^2. Constraining the albedo response to transitions between trees and crops/grasses from the models with satellite-derived data leads to an increase in this range; however after excluding two models with unrealistic conversion rates from trees to crops/grasses we obtain a revised multi-model mean estimate of -0.08 W/m^2 (with individual model results between -0.03 and -0.11 W/m^2). These numbers are at the lower end of the range provided by the IPCC AR5 (-0.15 +/- 0.10 W/m^2). The approach described in this study can be applied to other model simulations, such as those from CMIP6, especially as the evaluation diagnostic described here has been included in the ESMValTool v2.0.

Style Definition: Normal: Don't hyphenate
Style Definition: Heading 1: Don't hyphenate
Style Definition: Heading 4: Don't hyphenate
Style Definition: Line Number
Style Definition: Placeholder Text
Style Definition: Comment Reference
Style Definition: Unresolved Mention
Style Definition: Betreff: Don't hyphenate
Style Definition: Bullets: No bullets or numbering, Don't hyphenate
Style Definition: Header: Suppress line numbers, Don't hyphenate
Style Definition: Kontakt: Don't hyphenate
Style Definition: Name: Don't hyphenate
Style Definition: Copernicus_Word_template: Don't hyphenate
Style Definition: List Paragraph: Don't hyphenate
Style Definition: Balloon Text: Don't hyphenate
Style Definition: Equation: Don't hyphenate
Style Definition ... [2]
Style Definition ... [1]
Style Definition: Comment Subject: Don't hyphenate
Formatted: Width: 21 cm
Deleted: Radiative Forcing
Deleted: Radiative Forcing.
Deleted: 13
Deleted: Radiative Forcing
Deleted: albedo variations due to
Deleted: ranging between
Deleted: and
Deleted: 22
Deleted: 07
Deleted: ,
Deleted: 11
Deleted: 04
Deleted: 16
Deleted: on
Deleted: a diagnostic enabling the reproduction of the model
Deleted: part
Deleted: 1¶

1 Introduction

The landscape transformations imposed by anthropogenic activities have the potential to modify the climate (Foley *et al.*, 2005; Mahmood *et al.*, 2014). Since pre-industrial times, important Land Cover Changes (LCC) have especially led to the replacement of forests by shorter vegetation types such as crops and grasses over large inhabited areas (Ramankutty and Foley, 1999; Pongratz *et al.*, 2008; Hurtt *et al.*, 2011; Kaplan *et al.*, 2011). Associated alterations of land surface properties such as albedo, roughness and evaporative fraction have modified climate conditions through the so-called biogeophysical effects (Pongratz *et al.*, 2010; de Noblet-Ducoudré *et al.*, 2012; Lejeune, Seneviratne and Davin, 2017). The overall climate impact of the biogeophysical effects of historical LCC remains a matter of debate (Pitman *et al.*, 2009; de Noblet-Ducoudré *et al.*, 2012; Lejeune, Seneviratne and Davin, 2017; Duveiller *et al.*, 2018) due to uncertainties regarding the magnitude of the imposed land-cover perturbations (Schmidt *et al.*, 2012), the resulting alterations in land surface properties, the interplay between radiative (related to albedo) and non-radiative processes (related to changes in evaporative fraction and roughness), and the influence of atmospheric feedbacks and non-local effects (Winckler, Reick and Pongratz, 2017; Winckler *et al.*, 2019). Concerning the surface albedo more specifically, model studies concluded that historical LCC have led to large-scale increases in this variable (Betts *et al.*, 2007; Boisier *et al.*, 2013) because trees have a lower albedo than shorter vegetation types, especially in the presence of snow (Cescatti *et al.*, 2012; Li *et al.*, 2015). This has resulted in a cooling effect, and climate models have simulated an associated global Radiative Forcing (RF) close to -0.2 W/m^2 (Betts *et al.*, 2007; Davin, de Noblet-Ducoudré and Friedlingstein, 2007; Pongratz *et al.*, 2009). However, Myhre, Kvalevåg and Schaaf (2005) and Kvalevåg *et al.* (2010) have argued that climate models usually overestimate the albedo difference between natural vegetation and croplands in comparison to satellite-derived observational evidence. This is consistent with the weaker radiative forcing of -0.09 W/m^2 due to anthropogenic land cover change found by Myhre, Kvalevåg and Schaaf (2005), after combining a radiative transfer model with reconstitutions of past albedo changes based on satellite observations of the current vegetation land cover and its surface albedo, as well as a data set for potential natural vegetation. The Fifth Assessment Report (AR5) of the IPCC overall estimated that LCC since 1750 have rather led to a RF of -0.15 +/- 0.10 W/m^2 (G. Myhre *et al.*, 2013). A substantial spread in the albedo response to historical LCC has also been identified amongst the models participating in the LUCID project (de Noblet-Ducoudré *et al.*, 2012). The diversity of model parameterisations was estimated to be responsible for about half of it, while the remaining uncertainties result from differences in the magnitude of the prescribed land cover.

More recent model intercomparison efforts such as the fifth phase of the Coupled Model Intercomparison Project (CMIP5, Taylor, Stouffer and Meehl, 2012) offer new opportunities to assess the magnitude of these model disagreements, as well as our understanding of the impact of historical LCC on albedo and the associated RF. Nevertheless, such an investigation is complicated by the facts that the modelling groups participating in CMIP5 have not provided data on the albedo of specific land cover types but only mean albedo values over grid cells, which often contain various land cover types. Only a few modelling groups have conducted experiments to isolate the historical land use forcing. In parallel to recent model developments, studies giving insights from satellite data on the climate effect of LCC have been published (Li *et al.*, 2015;

Formatted: Outline numbered + Level: 1 + Numbering Style: 1, 2, 3, … + Start at: 1 + Alignment: Left + Aligned at: 0 cm + Indent at: 0,63 cm

Formatted: English (UK)

Formatted: English (UK)

Formatted: English (UK)

Formatted: French (Switzerland)

Formatted: English (UK)

Formatted: English (UK)

Formatted: English (UK)

Formatted: English (UK)

Formatted: English (UK)

Deleted: (Betts *et al.*, 2007; Edouard L. Davin, de Noblet-Ducoudré and Friedlingstein, 2007; Pongratz *et al.*, 2009)

Deleted: Myhre, Kvalevåg and Schaaf (2005)

Deleted: Kvalevåg *et al.* (2010)

Deleted: By

Deleted: , Myhre, Kvalevåg and Schaaf (2005) rather found a RF due to anthropogenic vegetation changes of -0.09 W/m^2 since pre-agriculture times. Consequently, the Fifth Assessment Report (AR5) of the IPCC

Deleted: (Myhre *et al.*, 2013)

Formatted: English (UK)

Deleted: Taylor, Stouffer and Meehl, 2012)

Deleted: -

Deleted: accounting for

Deleted: heterogeneity, and that

Deleted: of them

Deleted: isolating

Formatted: English (UK)

Deleted: 2¶

Alkama and Cescatti, 2016; Duveiller, Hooker and Cescatti, 2018b). They provide high-resolution information on the potential changes in various surface variables in response to land-cover transitions, which constitutes a very good benchmark to evaluate how this aspect is represented in climate models. The analyses described in this study thus rely on both climate model runs and satellite-based observational datasets to pursue two main objectives: 1) the validation of a methodology to systematically evaluate the representation of the surface albedo difference resulting from conversions between the dominant land cover classes in climate models (i.e., trees and crops/grasses) in standard climate model runs (such as from CMIP), with the view to be integrated in the ESMValTool v2.0 (Eyring *et al.*, 2020), and 2) the assessment of the Radiative Forcing from historical LCC using historical CMIP5 model simulations as well as observations to constrain model biases.

This study is therefore divided in several parts. First, we present the employed methods and data. In particular, we introduce a new methodology to extract the surface albedo for two different land cover classes (trees or crops/grasses), or the potential albedo change caused by conversions between these land cover classes, in simulations for which climate variables are only available at the grid cell level (Section 2). Second, we evaluate how well this methodology performs by using climate model simulations that also provide sub-grid cell albedo values for specific underlying land-cover types (Section 3) as a testbed. Third, we apply this approach to CMIP5 simulations to extract the surface albedo where the underlying vegetation is either trees or crops/grasses, as well as the surface albedo change due to transitions between these land cover classes simulated for present-day conditions, and compare the obtained results to satellite-derived reference data (Section 4). Fourth, we reconstruct the surface albedo changes since preindustrial times in CMIP5 models, and calculate the associated RF (Section 5). We also discuss the spread in the obtained model results in light of the biases identified in Section 4, and apply an observational constraint based on satellite-derived evidence to refine our estimates of the RF from historical LCC. Eventually, we compare our findings to those of previous studies, and discuss their limitations as well as potential for follow-up analyses (Section 6).

2 Methods and Data

2.1 Observational data

2.1.1 Albedo of land-cover classes

In this study we evaluate the surface albedo simulated by climate models, for each month and for two land-cover classes: crops/grasses (merged into one single land cover class) and trees, using reference estimates obtained from satellite measurements. It is important to note that in the analysed models as well as in satellite products the surface albedo is influenced by both the vegetation canopy and the soil reflectance, with the latter contribution being especially important in regions or periods where the Leaf Area Index is low. For the sake of simplicity, in this study the formulation "albedo of a specific land cover class" is used while referring to this mixed contribution of the soil and canopy to the surface albedo.

The observed surface albedo for both trees and crops/grasses is derived using the 300 meter-resolution land cover information provided by GlobCover v2.3 (Arino *et al.*, 2012), collected between January 2005 and June 2006, in combination with the

Formatted: Italian

Deleted: of

Deleted: specific

Deleted: and

Deleted:)

Deleted: information is

Deleted: as a testbed

Deleted:).

Deleted: of

Deleted: and

Deleted: the previous step

Formatted: Outline numbered + Level: 1 + Numbering Style: 1, 2, 3, … + Start at: 1 + Alignment: Left + Aligned at: 0 cm + Indent at: 0,63 cm

Deleted: for the albedo of land-cover classes and the albedo changes associated to land-cover transitions

Formatted: Outline numbered + Level: 3 + Numbering Style: 1, 2, 3, … + Start at: 1 + Alignment: Left + Aligned at: 0 cm + Indent at: 1,27 cm

Deleted: albedo of

Deleted: against

Deleted: To derive them, we

Deleted: 3¶

mean of the white-sky (bi-hemispherical) and black-sky (directional-hemispherical) shortwave albedo data at 0.05°-resolution from GlobAlbedo (Lewis *et al.*, 2012), available at monthly timescale for the 1998-2011 period. An optimal estimation approach and a gap-filling technique based on the MODIS surface anisotropy dataset were used to integrate data derived from the Advanced Along-Track Scanning Radiometer (AATSR), SPOT4-VEGETATION, SPOT5-VEGETATION2, and MERIS instruments (Lewis *et al.*, 2013; Muller *et al.*, 2013). GlobAlbedo products generally showed good agreement with estimates from MODIS (global R^2 of 0.85) and were assessed to be of very good quality overall; problems associated with snow detection were identified but lead to most significant artifacts at very high latitudes (>70°, Muller *et al.*, 2013).

To extract the albedo from specific land-cover types at a resolution of 2° (i.e., approximately equal to that of the model simulations), the GlobCover original data are first regridded from their original 300-m resolution to a regular 0.0025°-grid. We also group some classes provided in the detailed classification from GlobCover into two broad land cover classes (trees and crops/grasses), which are comparable to those for which the land cover fraction was reported by CMIP5 modelling groups. Details on how this grouping was performed are provided in Table S1. Then, for each grid cell of the GlobAlbedo dataset which is occupied by at least 95% by either trees or crops/grasses according to the GlobCover product, the seasonal cycle of albedo for this specific land cover type is approximated from the monthly albedo climatology for this grid cell, computed over the full period covered by GlobAlbedo. The results are then aggregated at 2° resolution, i.e. for each 2° grid cell the albedo climatology of a specific land cover type is derived by calculating area-weighted averages over the 0.05°-resolution grid cells it contains, and for which a land cover-specific seasonal cycle of albedo was previously identified. Although we haven't considered the so-called "mosaic" classes representative of heterogeneous landscapes in our analysis, the employed 95% threshold means that up to 5% of each selected 0.05° grid cell may contain other land cover types than those belonging to the tree or crop/grass classes, thus potentially preventing from retrieving their exact albedo values.

2.1.2 Albedo changes associated with land-cover transitions

The dataset of Duveiller, Hooker and Cescatti (2018a) – hereafter referred to as D18 – was used to evaluate the potential monthly surface albedo changes arising from land-cover transitions between trees and crops/grasses as simulated by CMIP5 models for present-day conditions. This 1°-resolution observational dataset was derived by "unmixing" the monthly albedo climatology over the 2008-2012 period from collection v005 of the NASA's MODerate-resolution Imaging Spectroradiometer (MODIS) MCD43C3 product (Schaaf *et al.*, 2002), using land cover information for the year 2010 from the ESA-CCI land-cover dataset (ESA Land Cover CCI Product User Guide Version 2. Tech. Rep., 2017, available at: http://maps.elie.ucl.ac.be/CCI/viewer/download/ESACCI-LC-PUG-v2.5.pdf). Their methodology is based on a "space-for-time" analogy, i.e. it assumes that albedo changes that would arise from a land cover transition from trees to crops/grasses, for example, can be approximated by spatial differences between albedo values of trees and crops/grasses over neighbouring areas, assuming the two land cover classes experience a similar background climate. The albedo product that served as input to construct the D18 dataset had been filtered for quality using the provided quality flags; the underlying logic was to favour higher quality retrieval without excluding too many values.

Deleted: comparable
Deleted: were
Deleted: at
Deleted: °. For
Deleted: spatial
Deleted: was then
Deleted: by
Deleted: to
Deleted: Duveiller, Hooker and Cescatti (2018a) – thereafter referred to as D18 – was used to evaluate the albedo changes associated to land-cover transitions between trees and crops/grasses in CMIP5 models. This
Deleted: NASA
Formatted: Font color: Auto, English (UK)
Deleted: http://maps.elie.ucl.ac.be/CCI/viewer/download/ESACCI-LC-PUG-v2.5.pdf).
Deleted: which can therefore be assumed to experience similar background climates. We used the version of the dataset from D18 that is based on a generic vegetation classification (IGBPgen) in four land cover classes: trees, shrubs, crops/grasses and savannas
Formatted: English (US)
Deleted: 4¶

We used a version of the D18 dataset that is based on a generic vegetation classification (IGBPgen) with only four land cover classes: trees, shrubs, crops/grasses and savannas. Imprecisions in land cover datasets are mostly confined to misclassifications between land cover types within these broad classes (e.g., between two types of trees) or the difficulty to properly identify medium-sized or mixed-type vegetation (i.e., shrub or savanna-like, see for example Bontemps *et al.*, 2011). In contrast, these products are best at distinguishing very distinct land cover types such as trees and crops/grasses. Therefore, the satellite-derived albedo values of these two broad classes (retrieved following the methodology presented in Section 2.1.1) as well as their differences (obtained from the D18 data) are characterised by relatively low uncertainties. Cescatti *et al.* (2012) had overall identified a slight underestimation (by 0-0.03) of the MODIS albedo compared to in situ data from FLUXNET (Baldocchi *et al.*, 2001) for a dozen of crops/grasses sites in the northern mid-latitudes, but it is difficult to exactly quantify the biases of satellite-based albedo products as there does not exist a sufficiently extensive network of in situ measurements to serve as a benchmark.

For the part of the analysis in which we estimate the observation-constrained RF associated with historical LCC in CMIP5 simulations, we used an extended version of the dataset originally presented by D18 that has a broader spatial coverage in order to increase the spatial overlap between model and observational results. The product from D18 was gap-filled by training a random forest classifier to reproduce the data according to similarities in local climate, and then using the climate information to predict the albedo changes due to specific land-cover transitions where gaps existed in the data, following the methodological steps described by Duveiller *et al.* (2020). Some precautions were taken to ensure that these predicted outputs remain realistic. First, all areas in which neither of the two land cover classes involved in a given transition are present were removed. Second, the random forest is only used for interpolation, i.e. only using combinations of climate indicator values that are actually observed for the considered transition. Finally, a clear systematic bias of the classifier was corrected by applying a simple linear regression.

2.2 Climate model simulations from CMIP5

In this study, we reconstruct two different quantities in CMIP5 models: 1) the simulated present-day albedo of trees and crops/grasses, to evaluate the albedo change arising from a potential transition between these two classes against observational data, and 2) the historical surface albedo changes associated with transitions between trees and crops/grasses, followed by an assessment of their consequences in terms of Radiative Forcing.

The simulated monthly surface albedo climatology for trees and crops/grasses under present-day conditions is reconstructed from historical "all-forcings" simulations of 16 CMIP5 models (Taylor, Stouffer and Meehl, 2012) for which the required information on land cover, downwelling shortwave radiation, upwelling shortwave radiation and snow cover fraction is available (see Section 2.3.1). A list of these models as well as those included in further parts of the analysis is available in Table S2. Land fractions covered by crops, grasses and pasture were provided separately by CMIP5 modelling groups, but were considered as one land cover class (crops/grasses) in this study to ensure consistency with the observational data from D18. Present-day surface albedo values and snow cover fractions are extracted from the last five-year period common to all

Deleted: ¶
The spatial coverage of the data from D18 is limited to the areas where there is a joint presence of the two vegetation classes of interest for a given land cover transition (e.g. forests to grasslands/croplands when considering a typical deforestation) over a local area of roughly 5 by 5 km. This is often not an issue, since many LCC generally occur in regions where both target and source classes already occur. However, it does limit the area over which the data can be confronted with model results, and it precludes exploring the possibilities of analysing new land cover change trajectories (e.g. planting trees in areas where none currently exist). Therefore, for the part of the analysis in which we estimate the observation-constrained RF associated to

Deleted: (Duveiller *et al.*, 2020). The gap-filling approach employed to derive it consisted in

Deleted: .

Deleted: types

Formatted: Outline numbered + Level: 2 + Numbering Style: 1, 2, 3, … + Start at: 1 + Alignment: Left + Aligned at: 0 cm + Indent at: 0,74 cm

Deleted: We

Deleted: from

Deleted: as well as

Deleted: in

Formatted: Font color: Auto

Deleted: of 13 CMIP5 models for which the required information on land cover, downwelling shortwave radiation, upwelling shortwave radiation and snow cover fraction is available (see Section 2.3.1 for a description of the reconstruction methodology). Land fractions covered by crops, grasses and pasture are provided separately by CMIP5 models, but were grouped within one same land cover class for consistency with the observational data from D18. Present-day albedo values are extracted from the last five-year period common to all models (i.e., 2000-2004), to be as close as possible to the period covered by the observational data.

Deleted: 5¶

models (i.e., 2000-2004), i.e. spanning a period similar in length and as close as possible to that covered by the albedo dataset used in D18. For three models (GFDL-CM3, GFDL-ESM2G and GFDL-ESM2M), the snow cover fraction outputs were not available but have been calculated from the snow mass values following the technique suggested and validated by Qu and Hall (2007): the snow cover fraction is assumed to be 1 at locations where the snow mass equals 60 kg/m^2, and to evolve as a linear function of snow mass where it equals between 0 and 60 kg/m^2. If several ensemble members differing only in terms of their initial conditions were available for one specific model, their ensemble mean was considered in the analysis.

We also reconstructed the surface albedo changes associated with historical transitions between trees and crops/grasses between pre-industrial conditions (equivalent to those of 1860 in CMIP5 and extracted from the first 200 years of the "piControl" experiments), and the 1981-2000 time period of historical "all-forcings" experiments. The reconstruction algorithm is applied to all CMIP5 models for which the required information on land cover, downwelling and upwelling shortwave radiation is available for at least two ensemble members of the analysed experiments (see Section 2.3.2 for a description of the reconstruction methodology). Since GFDL-ESM2G and GFDL-ESM2M are two very similar versions of the same model with only one ensemble member each, we have treated them as ensemble members of the same model (referred to as GFDL-ESM2). In order to be able to compute the RF constrained by observations, the reconstructed historical albedo changes associated with transitions between trees and crops/grasses were regridded to 1°x1° resolution. We have focused on the transitions between trees and crops/grasses for consistency with the observational data of D18, but also assessed the sensitivity of our results when considering the historical impact of overall changes in tree cover (e.g., also including replacement of trees by shrubs or bare soil). Additionally, factorial experiments isolating the climate forcing of historical LCC were available for four models: CanESM2, CCSM4, GFDL-ESM2 and IPSL-CM5A-LR. These experiments constitute benchmarks to evaluate the reconstructed historical albedo changes; the validity of the reconstruction is thus discussed further below as well as in the Supplementary Material.

2.3 Principle of the reconstruction method

2.3.1 Reconstruction of the simulated present-day albedo of specific land-cover classes

The present-day albedo values from trees and crops and grasses (α_{tr} and α_{cg}) in CMIP5 historical simulations are reconstructed using an "unmixing" method similar to those previously applied to satellite-derived observational data to extract the land surface characteristics of specific land cover types including albedo (Li *et al.*, 2015; Chen and Dirmeyer, 2019), and notably to obtain the data from D18 used as a reference for the evaluation of CMIP5 models in this study. We include information on the land fraction covered by shrubs in the methodology, but do not reconstruct the albedo of this land cover class (α_{sh}) because of its limited spatial occurrence.

Concretely, for every land grid cell *i* we considered spatial windows of 25 grid cells (5 in both the latitudinal and longitudinal dimensions) and centred over *i*, hereafter referred to as "big boxes" (see Figure 1). Within each big box, for each month we thus have a sample of up to 25 values for albedo (α) and the land cover fractions occupied by each of the three considered land

Deleted: the reconstruction method was applied to

Deleted: .

Deleted: ¶
In Section 5, we present estimates of

Deleted: RF associated to historical deforestation in fifteen CMIP5 models. For this purpose, we first reconstruct the

Deleted: both

Deleted: and the data from D18

Formatted: Font: Times New Roman

Formatted: Outline numbered + Level: 2 + Numbering Style: 1, 2, 3, … + Start at: 1 + Alignment: Left + Aligned at: 0 cm + Indent at: 0,74 cm

Formatted: Outline numbered + Level: 3 + Numbering Style: 1, 2, 3, … + Start at: 1 + Alignment: Left + Aligned at: 0 cm + Indent at: 1,27 cm

Deleted: The present-day albedo values from trees and crops and grasses (α_{tr} and α_{cg}) are reconstructed in CMIP5 historical simulations using an "unmixing" method similar to those previously applied to satellite-derived observational data to extract the land surface characteristics of specific land cover types (e.g., Alkama and Cescatti, 2016), including albedo (Li *et al.*, 2015; Chen and Dirmeyer, 2019), and notably to obtain the data from D18 used as a reference for the evaluation of CMIP5 models in this study. We include information on the land fraction covered by shrubs in the methodology, but do not reconstruct the albedo of this land cover type (α_{sh}) because of their limited spatial occurrence.¶
¶

Formatted: Font: Times New Roman

Deleted: big boxes

Formatted: Font: Times New Roman

Deleted: a size of 5 times 5

Formatted: Font: Times New Roman

Deleted: centered

Formatted: Font: Times New Roman

Deleted: .

Formatted: Font: Times New Roman

Deleted: (α)

Formatted: Font: Times New Roman

Deleted: 6¶

cover classes (lcf_{tr}, lcf_{sh}, lcf_{cg}) over the same simulation period. Multi-linear regressions of α against lcf_{tr}, lcf_{sh} and lcf_{cg} are then performed in order to obtain α_{tr}, α_{sh} and α_{cg}.

Variations in snow cover lead to large variations in surface albedo, therefore we focus on the identification of the albedo of trees and crops/grasses over grid cells with a snow cover fraction less than 0.1 (considered as snow-free), or greater than 0.9 (considered as snow-covered). In each big box and for a given month, if the grid cell at the centre i is snow-free the regression is conducted by considering only snow-free grid cells following:

$$\alpha^{sf} = \beta_0^{sf} + lcf_{tr} \times \beta_1^{sf} + lcf_{sh} \times \beta_2^{sf} + lcf_{cg} \times \beta_3^{sf} \quad (1)$$

where lcf_{tr}, lcf_{sh}, and lcf_{cg} are vectors containing up to 25 values, the β coefficients are specific to each big box and each month, and the superscript sf stand for snow-free. Similarly, if i is snow-covered the regression is conducted by considering only snow-covered grid cells:

$$\alpha^{sc} = \beta_0^{sc} + lcf_{tr} \times \beta_1^{sc} + lcf_{sh} \times \beta_2^{sc} + lcf_{cg} \times \beta_3^{sc} \quad (2)$$

where the superscript sc stands for snow-covered.

α_{tr} and α_{cg} over the central grid cell i of the big box are eventually reconstructed by extrapolating the partial linear regression lines for cases where lcf_{tr}, lcf_{sh}, and lcf_{cg} are equal to 100% following, in case i is snow-free:

$$\alpha_{tr}^{sf}(i) = \beta_0^{sf} + \beta_1^{sf} \times 100\% \quad (3)$$

$$\alpha_{cg}^{sf}(i) = \beta_0^{sf} + \beta_3^{sf} \times 100\% \quad (4)$$

or, if i is snow-covered:

$$\alpha_{tr}^{sc}(i) = \beta_0^{sc} + \beta_1^{sc} \times 100\% \quad (5)$$

$$\alpha_{cg}^{sc}(i) = \beta_0^{sc} + \beta_3^{sc} \times 100\% \quad (6)$$

This reconstruction method can only perform well over big boxes with sufficient land cover information. Therefore, each predictor (lcf_{tr}, lcf_{sh}, lcf_{cg}) is only included in the regression (i.e., its corresponding term is included in Equation (1) or (2)) if its value is greater than 0 in at least two snow-free (if i is snow-free) or snow-covered grid cells (if i is snow-covered). Moreover, the regressions are only conducted in the big boxes that have at least 15 grid cells (either snow-free or snow-

Formatted ... [3]
Deleted: α
Formatted ... [4]
Formatted ... [5]
Formatted ... [6]
Formatted ... [7]
Formatted ... [8]
Formatted ... [9]
Deleted: α
Deleted: α
Formatted ... [10]
Formatted ... [11]
Deleted: α
Formatted ... [12]
Deleted: ¶ ... [13]
Formatted ... [14]
Deleted: has an important impact on
Formatted ... [15]
Deleted: and especially
Formatted ... [16]
Deleted: difference between forests and short vegetation types ... [17]
Formatted ... [18]
Deleted: inferior to
Formatted ... [19]
Deleted: and one for the grid cells where this variable is superior ... [20]
Formatted ... [21]
Deleted:):
Formatted ... [22]
Formatted ... [23]
Deleted: ↵ ... [24]
Moved down [1]: $lcf_{tr} \times \beta_1^{sc} + lcf_{sh} \times \beta_2^{sc} + lcf_{cg} \times \beta_3^{sc}$
Deleted: $\alpha^{sf} = \beta_0^{sf}$
Deleted: (
Formatted ... [25]
Deleted: (2)
Formatted ... [26]
Formatted ... [27]
Formatted ... [28]
Formatted ... [29]
Deleted: β
Formatted ... [30]
Deleted: and sc refer to
Formatted ... [31]
Deleted: and
Formatted ... [32]
Deleted: , respectively.
Formatted ... [33]
Moved (insertion) [1]
Formatted ... [34]
Deleted: α
Formatted ... [35]
Deleted: , α_{sh}
Formatted ... [36]
Deleted: α

covered) in which the sum of all the included predictors exceeds 90%. After this reconstruction few remaining albedo values which are physically impossible (i.e., either smaller than 0 or larger than 1) are filtered out. In a last step, grid cells for which the standard error of the regression is higher than 0.01, or where the land fraction covered by trees and crops/grasses is lower than 20% are discarded.

The potential surface albedo change associated with a transition between trees and crops/grasses $\delta\alpha_{tr\rightarrow cg}$ is eventually calculated by looking at the difference between the reconstructed albedo of trees and crops/grasses, for each grid cell where both values were derived. As the fraction covered by trees and crops/grasses covary, the error associated with this difference strongly decreases compared to those of the albedo values of single land cover classes. The applied filtering criteria thus differ in this case: We only discard grid cells for which both the land fraction covered by trees and crops/grasses are lower than 10% and where the standard error of the regression is higher than 0.001.

A diagnostic enabling the automated reconstruction of the albedo difference between trees and crops/grasses in CMIP simulations following the methodology described in this section has been implemented in the ESMValTool v2.0 (more details available in Eyring *et al.*, 2020).

2.3.2 Reconstruction of the simulated albedo changes due to historical deforestation

A similar approach based on local regression is used to reconstruct the simulated historical albedo changes associated with transitions between trees and crops/grasses that occurred between pre-industrial times and the 1981-2000 period ($\Delta\alpha_{tr\rightarrow cg}$). It has previously been used to derive local changes in temperature due historical LCC in CMIP5 simulations (Lejeune *et al.*, 2018). In this case, the spatial predictors used to explain historical albedo changes ($\Delta\alpha$) are the historical transition rate between trees and crops and grasses ($lcc_{tr\rightarrow cg}$), latitude (*lat*), longitude (*lon*), and elevation (*elev*), such that, for each month:

$$\Delta\alpha = \gamma_0 + lcc_{tr\rightarrow cg} \times \gamma_1 + lat \times \gamma_2 + lon \times \gamma_3 + elev \times \gamma_4 \quad (7)$$

where $lcc_{tr\rightarrow cg}$, *lat*, *lon* and *elev* are vectors containing up to 25 values and the γ coefficients are specific to each big box. The regressions are conducted in big boxes containing at least 15 land grid cells to improve the quality of the reconstruction (Figure 1). The albedo change associated with historical local transitions between trees and crops/grasses over the central grid cell *i* of a big box is then obtained by scaling the results of this local regression with the historical conversion rate from trees to crops/grasses experienced over i (compared with pre-industrial conditions):

$$\Delta\alpha_{tr\rightarrow cg}(i) = lcc_{tr\rightarrow cg}(i) \times \gamma_1 \quad (8)$$

Deleted:), and where
Deleted: Moreover, the
Deleted: reconstructed
Formatted ... [61]
Formatted ... [62]
Formatted ... [63]
Deleted: inferior to
Formatted ... [64]
Deleted: superior to
Formatted ... [65]
Deleted: As
Formatted ... [66]
Deleted: to increase the quality of the results of the ... [67]
Formatted ... [68]
Formatted ... [69]
Deleted: to
Formatted ... [70]
Formatted ... [71]
Deleted: derived
Formatted ... [72]
Deleted: . The
Formatted ... [73]
Deleted: slightly
Formatted ... [74]
Deleted: , as we
Formatted ... [75]
Deleted: (as the fraction covered by trees and crops/grasses ... [76]
Formatted ... [77]
Deleted: the albedo of these land cover types the standard error ... [78]
Deleted: also
Formatted ... [80]
Deleted: , which allows the automated application of the ... [81]
Formatted ... [79]
Formatted ... [82]
Deleted: Eyring *et al.*, 2019).
Formatted ... [83]
Formatted ... [84]
Formatted ... [85]
Deleted: derive
Formatted ... [86]
Deleted: to
Formatted ... [87]
Deleted: $\delta\alpha_{tr\rightarrow cg}$
Formatted ... [88]
Deleted: reconstruct
Formatted ... [89]
Deleted: in the regression
Formatted ... [90]
Deleted:),
Formatted ... [91]
Deleted: *lat*),
Formatted ... [92]
Deleted: *lon*),
Formatted ... [93]

An uncertainty range for $\Delta\alpha_{tr\rightarrow cg}$ is also computed by applying the regression to each ensemble simulation of a given model. Additionally, for each ensemble simulation and each big box, a jackknife resampling is conducted: As many times as there are land grid cells with non-missing values in the big box, an additional regression is computed after leaving out each time a different grid cell (Efron, 1982). The obtained estimates of $\Delta\alpha_{tr\rightarrow cg}$ thus amount to between 16 and 26 – depending on the number of land grid cells in the big box – multiplied by the number of ensemble members. We then retain the median of these estimates, which increases the robustness of our results by eliminating strong dependencies on single model grid cells.

2.4 Computation of the Radiative Forcing of historical conversions between trees and crops/grasses

The Radiative Forcing (RF), expressed here in W/m^2, is defined as the net change in the energy balance of the Earth system due to some imposed perturbation (G. Myhre *et al.*, 2013). In our case, this perturbation is a modification of albedo arising from land-cover changes, in particular transitions between trees and crops/grasses, which affects the amount of reflected shortwave radiation leaving the Earth system at the top of the atmosphere. By how much this amount changes depends on a so-called radiative kernel (Soden *et al.*, 2008), defined in this case as the differential response in outgoing shortwave radiation at the top of the atmosphere to an incremental change in surface albedo $\delta\alpha_s$ (Bright and O'halloran, 2019):

$$RF = -K_{\alpha_s} \times \delta\alpha_s \quad (9)$$

We employ here the monthly CERES-based albedo change kernel (CACK) v1.0. Based on a novel, simplified parameterisation of shortwave radiative transfer (Bright and O'halloran, 2019), it is driven with a 16-year (2001-2016) climatology of downwelling shortwave radiation values at the surface and the top of the atmosphere obtained from the Clouds and the Earth's Radiant Energy System (CERES) Energy Balance and Filled (EBAF) 1°-resolution products (CERES Science Team, 2018). CACK (hereafter also referred to as $K_{\alpha_s}^{CACK}$) is more easily understandable and easier to apply than kernels derived from climate models, while being able to mimick them more faithfully than five previously employed analytical, semi-empirical and empirical kernels (Bright and O'halloran, 2019). The reconstructed albedo changes caused by historical conversions between trees and crops/grasses $\Delta\alpha_{tr\leftrightarrow cg}$ are also monthly, therefore the associated annual mean $RF_{tr\leftrightarrow cg}$ can be written as follows:

$$RF_{tr\leftrightarrow cg} = -\frac{1}{12}\sum_{m=1}^{12} K_{\alpha_s,m}^{CACK} \times \Delta\alpha_{tr\leftrightarrow cg,m} \quad (10)$$

where the subscript m denotes monthly values.

We derive two types of RF estimates in the analysed CMIP5 models. For the first one ("unconstrained"), which is purely model-based, we used the $\Delta\alpha_{tr\rightarrow cg}$ from historical conversion rates between trees and crops/grasses that were derived with the reconstruction method described in Section 2.3.2. The second one is constrained by observations, and was computed by

Deleted: $\delta\alpha_{tr\rightarrow cg}$
Formatted: Font: Times New Roman
Formatted: Font: Times New Roman
Deleted: Alternatively, and as
Formatted: Font: Times New Roman
Deleted: one
Formatted: Font: Times New Roman
Formatted: Font: Times New Roman, English (UK)
Deleted: We
Formatted: Font: Times New Roman, English (UK)
Deleted: obtain
Formatted: Font: Times New Roman, English (UK)
Deleted: estimates of $\delta\alpha_{tr\rightarrow cg}$,
Formatted: Font: Times New Roman
Formatted: Font: Times New Roman, English (UK)
Formatted: Font: Times New Roman
Formatted: Font: Times New Roman
Formatted: Font: Times New Roman, English (UK)
Formatted: Font: Times New Roman
Formatted ... [106]
Formatted: Font: Times New Roman
Deleted: (Myhre *et al.*, 2013).
Formatted: Font: Times New Roman
Deleted: deforestation or re/afforestation
Formatted: Font: Times New Roman
Deleted: (Bright and O'halloran, 2019)
Formatted: Font: Times New Roman
Deleted: K_{α_s}
Formatted: Font: Times New Roman
Deleted: 11
Formatted: Font: Times New Roman
Deleted: We employ here the empirical parameterisation of the ... [107]
Formatted: Font: Times New Roman
Deleted: $RF_{tr\rightarrow cg} = 0.854 \times SW_s^{\downarrow} \times \delta\alpha_{tr\rightarrow cg}$ (13)¶
Formatted: List Paragraph
Deleted: $\delta\alpha_{tr\rightarrow cg}$
Deleted: using
Deleted: 9¶

combining the historical conversion rates implemented in the models $lcc_{tr \to cg}$ with the potential surface albedo change associated with a transition between trees and crops/grasses from D18 ($\delta\alpha^{D18}_{tr \to cg}$) such as:

$$\Delta\alpha^{constrained}_{tr \leftrightarrow cg,m} = lcc_{tr \to cg} \times \delta\alpha^{D18}_{tr \to cg,m} \quad (11)$$

and

$$RF^{constrained}_{tr \leftrightarrow cg} = -\frac{1}{12} \times lcc_{tr \to cg} \times \sum_{m=1}^{12} K^{CACK}_{\alpha_s,m} \times \delta\alpha^{D18}_{tr \to cg,m} \quad (12)$$

2.5 Additional simulations to evaluate the reconstruction method

We employ two additional offline simulations conducted with the Community Land Model version 4.5 (CLM4.5; Oleson *et al.*, 2013) to evaluate the ability of the reconstruction method presented in Section 2.3.1 to extract the simulated albedo of trees and crops/grasses. The simulations were conducted at 1.9°x2.5° resolution, forced by the CRUNCEP v4 atmospheric forcing dataset (Harris *et al.*, 2014) for the years 1997 to 2010, and we kept the 2002-2010 period from the analysis. The default land cover map of CLM4.5 was kept constant at the state of 2000 throughout the simulation period (Lawrence and Chase, 2007). Grid cells in CLM4.5 are divided into tiles of different land units (glacier, wetland, vegetated, lake, and urban); the vegetated land unit comprises tiles of different Plant Functional Types (PFTs) including several types of trees, shrubs, grasses and crops, which all receive the same atmospheric forcing. Surface albedo values were output for each tile in these simulations, enabling to extract a subgrid albedo value for each land cover class (trees or crops/grasses, similarly as in Malyshev *et al.*, 2015; Meier *et al.*, 2018). For each grid cell and each month, the albedo values for these two land cover classes are computed as the area weighted mean albedo across each PFT pertaining to the respective class over the analysis period. This reference value, later referred to as "subgrid" estimate, can then be compared to the reconstructed albedo values. The results of this evaluation are described in Section 3.

3 Evaluation of the methodology to reconstruct the simulated albedo of individual land cover classes

3.1 Reconstruction of the albedo of trees and crops/grasses

The reconstructed July albedo estimates of trees and crops/grasses are close to the subgrid reference values in the CLM4.5 simulations, for the grid cells where the reconstruction method yields results (Figure 2). The main patterns of the spatial variability of the albedo of both land cover classes of interest, such as their latitudinal variations, are captured by the reconstruction method. Globally the reconstructed and subgrid albedo estimates are highly correlated (R^2=0.91 for trees and 0.75 for crops/grasses). Differences between them indicate the "error" of the reconstruction, thus allowing to compute a global Root Mean Square Error (RMSE) that considers all grid cells for which a reconstructed estimate could be derived. For the month of July, the global RMSE equals 0.0085 in the case of trees and 0.0097 for crops/grasses. Locally, the error is higher

Deleted: LCC
Deleted: and
Deleted: to
Deleted: to obtain $\delta\alpha_{tr \to cg}$.
Formatted: Outline numbered + Level: 2 + Numbering Style: 1, 2, 3, … + Start at: 1 + Alignment: Left + Aligned at: 0 cm + Indent at: 0,74 cm
Deleted: In order
Formatted: Font: Times New Roman
Deleted: , we apply it to additional offline simulations conducted with the Community Land Model version 4.5 (CLM4.5; Oleson *et al.*, 2013) and compare its results to the subgrid signal of the respective land cover change (e.g., Malyshev *et al.*, 2015; Meier *et al.*, 2018).
Formatted: Font: Times New Roman, English (UK)
Formatted: Font: Times New Roman
Formatted: Font: Times New Roman, English (UK)
Deleted: neglecting
Formatted: Font: Times New Roman
Deleted: first five years
Formatted: Font: Times New Roman
Formatted: Font: Times New Roman, English (UK)
Deleted: Grid cells in CLM4.5 are divided into tiles of different land units (glacier, wetland, vegetated, lake, and urban). The vegetated land unit comprises tiles of different Plant Functional Types (PFTs), including several types of trees, shrubs, grasses and crops, all receiving the same atmospheric forcing. We analyse tile-level model output to extract a subgrid albedo value for each land cover class (trees or crops/grasses). For each pixel and each month, the albedo values for the different land cover classes are computed as the area weighted means albedo across each PFT pertaining to the respective class over the simulation period.
Formatted: Font: Times New Roman
Formatted: Font: Times New Roman, English (US)
Formatted: Font: Times New Roman
Formatted ... [108]
Formatted ... [109]
Deleted: 1
Deleted: The "error" of the reconstruction is shown by the ... [110]
Deleted: can be computed across
Deleted: 009
Deleted: 010
Deleted: (Table 1).
Deleted: 10¶

over some areas with stronger albedo gradients such as Western Europe, the Southeastern United States in the case of trees or Western Russia in the case of crops/grasses. Nevertheless, the absolute error rarely exceeds ~0.03, or ~20% of the subgrid values over these regions (Figure S1).

In January, the reconstructed albedo estimates still resemble closely the reference values from the subgrid model outputs (Figure 3). However, the presence of snow increases both the mean value and the spatial variability of albedo which results in higher RMSEs over grid cells located north of 40°N (0.037 for trees, respectively 0.0295 for crops/grasses as indicated in the right panel), leading to global RMSEs of 0.019, respectively 0.013. As a result, within one big box used for the reconstruction, the dispersion between the albedo values from individual grid cells is higher. This renders the extraction of the correct albedo values of specific land cover classes with the regression-based reconstruction method more difficult. The spatial coverage of the reconstruction method also diminishes during months with a higher snow cover, because our methodology excludes grid cells which are neither considered snow-free nor snow-covered from the reconstruction, as is the case in Western Europe or the Northeastern United States in January. The absolute error of the reconstruction method reaches a maximum of ~0.1 or ~30-40% over localised parts of Eastern Siberia during this month (Figure S2).

3.2 Reconstruction of the albedo change from deforestation

Overall, the reconstructed estimates of the July albedo change associated with deforestation also show a good correspondence with the subgrid reference values (Figure 4). The global RMSE increases up to 0.0189 in this case, because it is a combination of the errors from the reconstruction of the albedo of both trees and crops/grasses. The magnitude of this error needs to be assessed in relation to the local albedo difference between trees and crops/grasses. Previous studies using satellite observations have shown that this difference roughly ranges between 0.03 and 0.07 over mid-latitudes during summer (Li *et al.*, 2015; Duveiller, Hooker and Cescatti, 2018b). This means that in most regions the local difference between the reconstructed and subgrid estimates remains less than the albedo difference between forest and crops/grasses, but can attain similar magnitudes in some regions such as Western Europe or the Northeastern United States (Figure S3).

For January, the reconstructed and subgrid estimates of the deforestation-induced albedo change remain similar to each other (Figure 5), with a global RMSE that slightly increases to 0.025 and reaches 0.0505 on average north of 40°N. The relative error between the reconstructed and subgrid albedo values is similar as in January over localised tropical or subtropical areas where it can reach 80%, whereas it mostly remains limited to +/-10% over snow-covered regions (Figure S4). This is because the absolute error remains of similar magnitude as in July in snow-free regions, while the albedo change induced by deforestation increases in the presence of snow due to the snow-masking effect of forests.

Overall, the reconstruction method yields similar estimates of the absolute albedo of trees and crops/grasses (Section 3.1), and a similar albedo difference between these two land cover classes as the subgrid reference values in the analysed CLM4.5 simulations. It is nevertheless associated with an error that varies with the season and more particularly with the presence of snow. These uncertainties introduced through the reconstruction method need to be kept in mind in the upcoming section,

Deleted: 2), although the global RMSEs are higher (0.019 for trees, and 0.013 in the case of crops/grasses, see Table 1). These higher errors are due to

Deleted: over larger areas, which leads to

Deleted: in

Deleted: Overall, the reconstruction method yields estimates of the albedo of trees and crops/grasses which are similar to the subgrid reference values in the analysed CLM4.5 simulations. This suggests that the reconstruction method can be applied to model runs produced with CMIP5 models, in order to estimate the albedo that they simulate for both of these land cover classes during present-day, and eventually compare it with observational reference data.¶
¶

Formatted: Outline numbered + Level: 2 + Numbering Style: 1, 2, 3, … + Start at: 1 + Alignment: Left + Aligned at: 0 cm + Indent at: 0,74 cm

Deleted: to

Deleted: 3

Deleted: 019

Deleted: associated to

Deleted: albedo

Deleted: As a result,

Deleted: can be as large as

Deleted: overall

Deleted: 4

Deleted: (Table 1).

Deleted: can reach 80%

Deleted: , however

Deleted: Overall, these results suggest that the reconstruction method can be applied in order to estimate the simulated deforestation-induced albedo change in CMIP5 models; however the interpretation of the results should be conducted with caution, keeping in mind the magnitude of the error associated to the reconstruction, especially over snow-free regions.¶

Deleted: 11¶

where the reconstruction method is applied to CMIP5 simulations and the resulting albedo estimates of trees, crops/grasses as well as the difference between the two are compared to satellite-derived reference values.

4 Present-day potential albedo changes associated with a transition from trees to crops/grasses in CMIP5 models and observations

4.1 Evaluation of the present-day albedo of trees and crops/grasses in CMIP5 models

4.1.1 Albedo of trees

The reconstructed albedo of trees varies considerably across the analysed CMIP5 models for the month of July, especially over the mid-to-high latitudes (Figure 6). Estimates derived from CanESM2 and the models from the MPI suite (MPI-ESM-LR, MPI-ESM-MR, MPI-ESM-P) show the highest similarities with the observed ones. The climate models which use the CLM as a land surface scheme (CCSM4, CESM1-CAM5, CESM1-FASTCHEM, CESM1-WACCM, NorESM1-M, NorESM1-ME) as well as MIROC5 all underestimate the albedo of trees over mid-to-high latitudes. They indeed simulate values lower than 0.1, whereas the estimates derived from observational data always remain above 0.1, and mostly range between 0.12 and 0.16 over these regions. On the other hand, the models from the GFDL suite (GFDL-CM3, GFDL-ESM2G, GFDL-ESM2M) exhibit higher tree albedo values than the in the reference data, especially over tropical regions where the overestimation can be as high as ~0.1. Lastly, our results indicate strong spatial variations in the case of the MIROC-ESM and MIROC-ESM-CHEM models, with negative biases over the high latitudes and Southeast Asia. The magnitude of these differences between reconstructed and reference estimates is significantly higher than the reconstruction error which has been assessed from the analysis of the CLM4.5 simulations (global RMSE of 0.0085, see Section 3.1).

For January, albedo increases over the regions where snow is present are reflected in the reference data (Figure 7). A latitudinal gradient can especially be noted, as the values derived from GlobCover and GlobAlbedo typically barely exceed 0.15 in Western Europe, but are higher than 0.3 in Scandinavia and even reach ~0.5 in Northern Siberia. Our results show that CanESM2 and the climate models using the CLM also simulate higher albedo values over snow-covered regions, with values that remain within the range indicated by observations for this time of the year. However, the models from the GFDL suite and especially GFDL-CM3 present an overestimation of these quantities, a behaviour that is even more pronounced in MIROC5 which exhibits values exceeding 0.5 north of ~50°N, and even reaching ~0.7 in areas located close to the Arctic ocean. Such biases have already been reported for GFDL-ESM2M and MIROC5 and linked to unrealistic parameterisations of snow canopy and vegetation masking (Thackeray, Fletcher and Derksen, 2015). They are significantly higher than the typical error of the reconstruction method identified for this month north of 40°N (~0.037). Unfortunately, in the case of MIROC-ESM, MIROC-ESM-CHEM and the models from the MPI suite (MPI-ESM-LR, MPI-ESM-MR and MPI-ESM-P) the spatial coverage of the reconstruction method is too low to be able to draw meaningful comparisons with observations over snow-covered areas.

Deleted: to

Formatted: Outline numbered + Level: 1 + Numbering Style: 1, 2, 3, … + Start at: 1 + Alignment: Left + Aligned at: 0 cm + Indent at: 0,63 cm

Formatted: Outline numbered + Level: 2 + Numbering Style: 1, 2, 3, … + Start at: 1 + Alignment: Left + Aligned at: 0 cm + Indent at: 0,74 cm

Formatted: Outline numbered + Level: 3 + Numbering Style: 1, 2, 3, … + Start at: 1 + Alignment: Left + Aligned at: 0 cm + Indent at: 1,27 cm

Deleted: 5

Deleted: those obtained by combining the observational datasets GlobAlbedo and GlobCover.

Deleted: inferior to

Deleted: The magnitude of the underestimation is in that case significantly higher than the reconstruction error which has been assessed from the analysis of the CLM4.5 simulations (global RMSE of 0.009, see Section 3.1).

Deleted: observations show that the

Deleted: of trees

Deleted: 6

Deleted: On the other hand, MIROC5 tends to overestimate albedo under the presence of snow, with

Deleted: Unfortunately, in the case of MIROC-ESM, MIROC-ESM-CHEM and the models from the MPI suite

Deleted: 12¶

4.1.2 Albedo of crops/grasses

There are also important variations among the simulated albedo of crops and grasses in the CMIP5 models we have analysed, pointing to significant model biases in comparison to observation-derived reference estimates. Overall, the models that employ the CLM tend to underestimate this quantity over large parts of the tropics and the mid-latitudes in the Northern Hemisphere in July, with reconstructed albedo values of ~0.13-0.14 whereas observations rather indicate values of at least 0.15 and even approaching 0.25 over the Sahel and Central Asia (Figure 8). This discrepancy appears less pronounced over the tropical parts of Africa and America located in the Southern Hemisphere, despite the lower availability of observational estimates over these regions. Our results also reveal that MIROC5 more systematically underestimates the albedo of crops/grasses, which remain less than 0.15 worldwide in this model. In contrast, the models from the MPI suite simulate albedo values that are consistently greater than those of the observations, exceeding 0.2 over large regions of the world. These overestimations are often higher in the GFDL models, especially over Central Asia, the southern part of South America or the southern tip of Africa, although these three models present an opposite behaviour over equatorial regions of America and Africa with remarkably low albedo values. Importantly, these numerous reported differences between the reconstructed model estimates and the reference values from observations are significantly higher than the error of the reconstruction method derived from the analysis of the CLM4.5 simulations (~0.01 in the case of crops/grasses for the month of July, see Section 3.1). The albedo values simulated by MIROC-ESM and MIROC-ESM-CHEM appear closer to the observational estimates over the regions where those are available. Lastly, the spatial coverage of the reconstruction is low in the case of CanESM2, which prevents drawing robust conclusions for this model.

Results for the month of January indicate that the models that include the CLM, as well as MIROC5 and those from the MPI and GFDL suites all represent the increase in the albedo of crops/grasses over snow-covered areas which is indicated by observational estimates (Figure 9). The limited spatial coverage of the latter over the high latitudes however makes it difficult to evaluate whether the magnitude of this increase is correctly represented. Over the tropical regions, the models including the CLM simulate an opposite pattern compared to that shown for the month of July, i.e. an underestimation of the albedo of crops/grasses in the Southern Hemisphere but more realistic estimates in the Northern Hemisphere. This suggests that these models simulate too high variations of the annual cycle for this variable over tropical regions.

4.2 Evaluation of the albedo changes induced by a transition from trees to crops/grasses in CMIP5 models

The observational dataset from D18 indicates that deforestation leads to a higher local albedo over each region of the world it covers, with some spatial variations in the magnitude of this increase. In July, this increase is lowest (<0.01) over Eastern Asia and Southwestern Siberia, and highest (~0.1) over the western part of North America (Figure 10). Our reconstructions indicate that most of the analysed CMIP5 models simulate the deforestation-induced albedo increase over most regions of the world. However, there are biases that are significantly higher than the typical error of the reconstruction method derived from its evaluation on CLM4.5 simulations (~0.02 in July, see Section 3.2). At this time of the year, the CanESM2 and MIROC5

Formatted: Outline numbered + Level: 3 + Numbering Style: 1, 2, 3, … + Start at: 1 + Alignment: Left + Aligned at: 0 cm + Indent at: 1,27 cm

Deleted: 6

Deleted: inferior to

Deleted: superior to

Deleted: the

Deleted: (

Deleted: suite

Deleted: 8

Deleted: namely

Formatted: Outline numbered + Level: 2 + Numbering Style: 1, 2, 3, … + Start at: 1 + Alignment: Left + Aligned at: 0 cm + Indent at: 0,74 cm

Deleted: .

Deleted: 8

Deleted: (

Deleted: 019

Deleted: and 0.025 in January

Deleted: ¶
For

Deleted: month of July

Deleted: 13¶

models show the closest resemblance to the observational reference data, although they overestimate the albedo increase due to deforestation over some regions such as Eastern Asia. As a result of their strong overestimation of the albedo of crops/grasses (see Section 4.1), the models from the MPI suite exhibit significant positive biases in the deforestation-induced albedo increases across the globe in July, with values reaching ~0.1 over large areas. Positive biases of a lower magnitude, although still significant, are also found over specific regions in the models using the CLM as a land surface scheme, consistently with the evaluation of the subgrid albedo difference in CLM4.5 of Meier *et al.* (2018). Over the mid-latitudes, this is due to the underestimation in the albedo of trees, whereas it can be related to the too high albedo of crops/grasses over the tropical regions of the Southern Hemisphere for this time of the year. Lastly, the MIROC-ESM, MIROC-ESM-CHEM and GFDL models exhibit a strong spatial variability in the reconstructed signals. In contrast with the observational data which consistently indicate an increase in albedo after deforestation, our estimates suggest that the former two simulate the opposite behaviour over extensive areas of Central Asia, but also the western parts of Canada and the United States and south of 25°S in Africa, America and Western Australia. As for the GFDL models, similarly to the models from the MPI suite they exhibit an overestimation of the albedo of crops/grasses in July (Section 4.1.2), but also an overestimation of the albedo of trees in many regions and both tend to compensate in some regions. This leads to the described spatial variability in the biases associated with the deforestation-induced albedo increase, which can even become negative over Europe although their limited magnitude suggests to interpret them with caution, in light of the error of the reconstruction method. The negative biases over the equatorial band can however directly be linked to the very low albedo of crops/grasses reported in these regions and for these models (Section 4.2.2).

Compared to July, the observations of D18 for the month of January indicate a higher albedo increase following deforestation over the mid-to-high latitudes where snow is present, the magnitude of which is overestimated by ~0.05-0.1 by the CMIP5 models including the CLM (Figure 11). This is slightly higher than the typical error of the reconstruction method (~0.05 north of 40°N), and in line with the findings of Meier *et al.*, 2018. These models also consistently simulate a localised, likely non-significant albedo decrease following deforestation over Eastern Europe, a feature that is not present in the observations. Strikingly, our results suggest that the MIROC-ESM and MIROC-ESM-CHEM models simulate strong albedo decreases (below -0.3) over large-snow covered regions at this time of the year, a behaviour that is in strong contradiction with what observational data indicate. In line with the overestimation of the albedo of trees over high latitudes represented by MIROC5, this model also simulates albedo decreases as a response to deforestation over parts of Europe.

5 Implications for the Radiative Forcing from historical deforestation

Our reconstructions of the RF from transitions between trees and crops/grasses since preindustrial times indicate a large spread within the CMIP5 models which were considered in this analysis (Figure 12), with estimates of the global mean RF ranging between 0 and -0.17 W/m^2. This dispersion is due to differences in two factors across the models: their local albedo responses to a transition between trees and crops/grasses, and the historical conversion rates between these two land cover classes that

Deleted: and the eastern part of North America.

Deleted: Meier *et al*. (2018)

Deleted: and

Deleted: Contrary to

Deleted: both of these models

Deleted: eastern

Deleted: 10). These models also consistently simulate a localised albedo decrease following deforestation over Eastern Europe, while this feature is not present in the observations.

Deleted: inferior to

Formatted: Outline numbered + Level: 1 + Numbering Style: 1, 2, 3, … + Start at: 1 + Alignment: Left + Aligned at: 0 cm + Indent at: 0,63 cm

Deleted: 11

Deleted: 22

Deleted: 14¶

the models simulate or prescribe (depending on whether they used a dynamic vegetation module or not). In Eq. (8), the former factor is represented by $\gamma_{1,x}$ and the latter by $lcc_{tr \to cg}$. Observation-constrained estimates of the RF from the historical conversion rates in CMIP5 models were obtained by replacing the reconstructed values of γ_1 by those from D18 (Figure 13, see also Sections 2.3.2 and 2.4 for more information on the methodology). The differences between the unconstrained and constrained RF values therefore reflect the model biases in the local albedo response to a present-day conversion from trees to crops/grasses, which have been described in Section 4.2 for a subset of the models considered here for the months of July and January. Hence, the constrained global RF estimates from the models using the CLM as a land surface scheme (CCSM4, CESM1-CAM5, CESM1-FASTCHEM, NorESM1-M) and those from the MPI suite (MPI-ESM-LR, MPI-ESM-MR, MPI-ESM-P) are less negative than the unconstrained estimates by 0.01-0.02, respectively 0.04-0.07 W/m^2, reflecting the fact that these models were found to overestimate the albedo increase via this land cover transition. On the other hand, the low albedo response exhibited by MIROC5 in snow-covered regions can be related to the more negative RF (by 0.01W/m^2) obtained for this model after constraining it with the observational data from D18. Similarly, the mix of albedo decreases and increases following a present-day transition from trees to crops/grasses that have been identified for MIROC-ESM both in January and July can also explain that the global reconstructed RF equals zero for this model, whereas it reaches -0.23W/m^2 after applying the same observational constraint. As for the GFDL-CM3 and GFDL-ESM2 models, the unconstrained global RF values become more negative by 0.05-0.06 W/m^2 once constrained with the observations from D18, reflecting the locally low or negative albedo sensitivity to deforestation described in Section 4.2 but also suggesting other important biases at very high latitudes, where the reconstructed model estimates could not be derived. Our results also suggest that the albedo change following a transition from trees to crops/grasses simulated by HadGEM2-ES is sensibly higher than in the observations from D18, as the unconstrained global RF of -0.01 W/m^2 is reduced to approximately zero after the observational constraint is applied. Lastly, the constrained and unconstrained estimates of the IPSL-CM5A-LR and IPSL-CM5A-MR models are very similar, suggesting that the albedo response to a conversion between trees and crops/grasses simulated by these models is close to the observed values.

Although it solely reflects the model spread in the historical conversion rates between trees and crops/grasses $lcc_{tr \to cg,x}$ the dispersion between the constrained estimates of the global RF is higher than between the unconstrained ones (Figure 14). This is due to two models in particular, for which the $lcc_{tr \to cg}$ values are outliers among the whole set of models, but which at the same time exhibit significant biases in their albedo response to these LCC. Thus, in the HadGEM2-ES model the historical conversion rates from trees to crops/grasses are approximately equal to zero everywhere on the globe (Figure S5), hence the corresponding constrained global RF too. However, because the albedo sensitivity to a transition from trees to crops/grasses of this model is stronger than in the observations, the unconstrained RF is slightly more negative (and reaches -0.01W/m^2). The unconstrained RF equals zero for MIROC-ESM, which is in line with a globally averaged albedo response to transitions between trees and crops/grasses that is also equal to zero, as described above in this Section. In contrast, this model also

Deleted: 10
Deleted: δ_1,
Deleted: $lcc_{tr \to cg}$
Deleted: δ_1
Deleted: 12
Deleted: .
Deleted: 06
Deleted: by
Deleted: 02W
Deleted: be linked to the fact
Deleted: 29W
Deleted: GFDL-CM3 and GFDL-ESM2
Deleted: lower
Deleted: constrained estimates are more negative that the constrained ones by as much as 0.09-0.1 W/m^2 for these two models. We identify the opposite behaviour for HadGEM2-ES, for which the
Deleted: once
Deleted: revealing an
Deleted: that
Deleted: $lcc_{tr \to cg}$,
Deleted: 13
Deleted: $lcc_{tr \to cg}$
Deleted: land cover changes.
Deleted: 15¶

exhibits the strongest constrained estimate (with -0.29 W/m^2) because of the strong historical conversion rates it simulates, which exceed 50% over large areas of Australia, North America, southeastern Brazil, Central Asia and southern Africa.

The extremely low, respectively high historical conversion rates from trees to crops/grasses in HadGEM2-ES and MIROC-ESM cast doubt on the global RF obtained for these two models. In Figure 14 we therefore also show the model spread after omission of the maximum and minimum values of both the unconstrained and constrained RF estimates. It is reduced from 0.15 to 0.08 W/m^2 after applying the observational constraint, which also leads to a slightly more negative model mean value (-0.08 W/m^2 instead of -0.05, note that the models including the same land surface scheme and land cover maps are considered as just one model for the computation of the mean).

For most CMIP5 models, our reconstructions indicate that the historical impact of conversions between trees and crops/grasses on albedo is very similar to that arising from all changes in tree cover (i.e., also including for example the replacement of trees by shrubs and bare soil, or vice-versa, see Figures S6-20). Moreover, we also find a similar effect for albedo variations from all LCC (i.e., also including transitions between shrubs, crops/grasses and bare soil) by comparing experiments with and without the land-cover forcing, available for four of the analysed models (CanESM2, CCSM4, GFDL-ESM2 and IPSL-CM5A-LR, see Figures S6, S7, S11 and S13). HadGEM2-ES is a notable exception (Figure S12), because it overall exhibits a decrease in tree cover comparable to that of other models, but which is not compensated by increases in the area covered by crops/grasses, shrubs or bare soil (not shown). Consequently, the reconstructed method does not capture the full RF from historical LCC for this model, which had been found by Andrews *et al.* (2017) to be extremely negative. Since it solely considers the transition between trees and crops/grasses, this method likely also slightly overestimates the RF for MPI-ESM-LR, MPI-ESM-MR and MPI-ESM-P (Figures S17-S19), because these three models represent an expansion of both forest and crops/grasses over high latitudes. Despite these limitations, our analysis shows that the reconstructed RF from historical transitions between trees and crops/grasses are overall good approximations of the RF from all LCC for most of the analysed CMIP5 models (see also Figure S21).

6 Discussion and conclusions

The conclusions that can be drawn from the presented analysis are manifold. First, we introduced a methodology to derive the albedo of trees and crops/grasses from Earth System model simulations that only provide mean albedo values over grid cells containing a mix of land cover classes. This "reconstruction" method employs multi-linear regressions to disentangle local information on land cover and albedo within moving windows ("big boxes") encompassing several grid cells. It assumes that spatial albedo variations between neighbouring trees and crops/grasses within a big box are good proxies of the potential albedo change arising from a transition between these two land cover classes. We then demonstrated that in the Community Land Model the estimated albedos of trees and crops/grasses from the reconstruction method are close to the values provided at the sub-gridcell level. Consequently, as a second step we reconstructed the present-day albedo of trees and crops/grasses in CMIP5 simulations for sixteen models, and compared the obtained results with reference values from observations. Despite

Deleted: 13

Deleted: 2

Deleted: 12

Deleted: 11

Deleted: 07

Deleted: land-cover changes

Deleted: land-cover changes for this model.

Deleted: land-cover changes

Formatted: Outline numbered + Level: 1 + Numbering Style: 1, 2, 3, … + Start at: 1 + Alignment: Left + Aligned at: 0 cm + Indent at: 0,63 cm

Deleted: methodology gives estimates of

Deleted: albedo

Deleted: that

Deleted: reference

Deleted: in simulations for which this information is available.

Deleted: thirteen

Deleted: 16¶

the relatively low spatial coverage of the reconstructed estimates in some models, especially over regions where snow is present, we were able to identify substantial model biases for the months of January and July which are significantly higher than the error of the reconstruction method. We found that they are reflected further in the representation of the albedo change induced by a transition between trees and crops/grasses in the same CMIP5 models. Finally, we investigated how such model biases influence the historical albedo change due to transitions between trees and crops/grasses as simulated by CMIP5 models, as well as the associated Radiative Forcing. To do so, we used another reconstruction methodology, already employed in previous studies, to assess how albedo has been modified as a result of the replacement of trees by crops/grasses since pre-industrial times in fifteen CMIP5 models (including most of those analysed in the previous step). We then derived the associated historical RF by using a recently published kernel, which constitutes of a simple parameterisation found to mimick the behaviour of climate models and applied to CERES radiation observations. An observational constraint was also applied to these estimates, by replacing the reconstructed albedo response to a conversion from trees to crops/grasses in the models by that of the observational dataset previously used for the model evaluation. The comparison of the unconstrained and observation-constrained RF in the individual models revealed differences reflecting some of the model biases that we had previously described. Moreover, the observational constraint leads to a multi-model mean RF associated with the historical replacement of trees by crops/grasses that is slightly reduced from -0.05 to -0.08 W/m^2, and a model range spanning from -0.03 and -0.11 W/m^2 after excluding two model outliers with unrealistically low or high historical conversion rates between trees and crops/grasses. Considering all variations in tree cover or even all LCC gives very similar results, because of the simplified representation of land cover in CMIP5 models.

Our RF estimates were derived with all-forcing simulations in which climate is evolving due to mostly other forcings (G. Myhre *et al.*, 2013), and thus are theoretically not exactly comparable with results from studies that assessed the impact of historical LCC in isolation from other forcings. However, our finding that the reconstructed albedo values are similar to those derived with LCC-only experiments conducted within CMIP5 (see Figures S6, S7 and S21) indicate that changes in background climate from other forcings have had little influence on the overall LCC-induced albedo changes over the 1860-2000 period, hereby confirming earlier similar conclusions (Boisier *et al.*, 2012; de Noblet-Ducoudré *et al.*, 2012). The identified range of -0.03 to -0.11 W/m^2 for the global RF is at the lower end of that of -0.15 +/- 0.10 W/m^2 provided by the IPCC AR5 (i.e., less negative than its best estimate, see Figure 14). This result confirms that the LCC forcing is unlikely to have played a large role historically for global mean impacts (G. Myhre *et al.*, 2013; Smith *et al.*, 2020), while still being important at the local to regional scales (Pongratz *et al.*, 2010; Boisier *et al.*, 2012; de Noblet-Ducoudré *et al.*, 2012). It is also lower than the estimates close to -0.2 W/m^2 from Betts *et al.*, (2007); Davin, de Noblet-Ducoudré and Friedlingstein (2007) and Pongratz *et al.* (2009). Myhre, Kvalevåg and Schaaf (2005) and Kvalevåg *et al.* (2010) had suggested that these climate model-based studies had overestimated the simulated albedo response to historical LCC. In this regard ,our study reveals that such an overestimation does exist for some CMIP5 models, but is not systematic across the analysed ensemble. Our model mean result is very close to, respectively slightly lower than those of Myhre, Kvalevåg and Schaaf (2005) and Ghimire *et al.* (2014), who both used satellite data to reconstruct past albedo changes and found RFs of -0.09 and -0.15 W/m^2 when

Deleted: a similar

Deleted: empirically based radiative kernel parametrisation.

Formatted: English (US)

Deleted: constrain

Deleted: purely model-based

Deleted: if one omits the influence of

Deleted: which have extremely

Deleted: , the model spread diminishes and the model mean value is slightly more negative due to the application of the observational constrain, overall leading to a mean estimate of -0.11 W/m^2 (between -0.04 and -0.16) for the RF due to the historical replacement of trees by crops/grasses.

Deleted: land-cover changes

Deleted: Our RF estimates are therefore directly comparable with those from previous model-based studies, although these considered the effect of all types of land-cover changes. In particular, the IPCC AR5 states that it is very likely that land use change since preindustrial times led to an increase of the Earth albedo with a RF of -0.15W/m^2 (Figure 13), thereby suggesting that the climate model-based studies from Betts *et al.* (2007), E. L. Davin, de Noblet-Ducoudré and Friedlingstein (2007), and Pongratz *et al.* (2009) – which provided numbers closer to -0.2 W/m^2 – had overestimated the simulated albedo response to historical land-cover changes (Myhre *et al.*, 2013). Although our study reveals that such an overestimation is not systematic in the analysed CMIP5 models, it still suggests that the RF from historical land-cover changes is at the lower end of the range provided by AR5 (i.e., rather less negative than its best estimate). Our model mean result is very close to that of Myhre, Kvalevåg and Schaaf (2005), who also constrained past albedo changes with satellite data and found a RF of -0.09 W/m^2, but considered all LCC since pre-agricultural times.¶
The remaining spread in our constrained RF estimates directly reflects the differences in the

Deleted: 17¶

considering all LCC since pre-agricultural times. It is also slightly less negative than – although within the uncertainty range – of the multi-model mean RF of -0.14 W/m^2 estimated within the Radiative Forcing Model Intercomparison Project (RFMIP) as part of the 6th phase of CMIP (CMIP6, Smith *et al.*, 2020), which also found that it would translate into an Effective Radiative Forcing of -0.09 W/m^2 after adjustment of the state of the troposphere (clouds, water vapour content, etc.).

Additionally, part of these differences and of the model spread identified in this study arises from different simulated historical conversion rates from trees to crops/grasses. Despite being based on the same Land Use History a product (LUHa, Hurtt *et al.*, 2011), the LCC trajectories in the analysed CMIP5 historical simulations reflect varying interpretations of this dataset. LUHa gives gridded information on annual transitions between four types of land use (primary land, secondary land, crop and pasture) for the 1500-2005 period, which were derived with the Global Land use Model (GLM) based on historical data. These transitions were especially designed to provide common reference land use trajectories for all historical CMIP5 simulations. The CMIP5 models may have however considered that primary and secondary land were either forests or crops/grasses, or even shrubs or bare soil, depending on the land cover distributions that were prescribed or simulated in a given region or under a given climate. These different interpretations of common land use input data contribute substantially to the spread in the albedo variations due to historical LCC. This result had already been identified for the models participating to the LUCID project (Boisier *et al.*, 2012), as well as more generally for the biogeophysical effect of future LCC on climate in RCP4.5 and RCP8.5 simulations from CMIP5 (Brovkin *et al.*, 2013; Davies-Barnard *et al.*, 2014; Di Vittorio *et al.*, 2014). Solutions have been put forward to reduce the room for interpretation of the imposed land cover forcing in future model intercomparison efforts, such as a direct coupling between the Integrated Assessment Models producing the land cover scenarios and the Earth System Models (Di Vittorio *et al.*, 2014), or the provision of more detailed land cover information (including the land cover fractions allocated to several specific land-use states) in the frame of CMIP6 (Lawrence *et al.*, 2016). These may bring the multi-model mean RF estimate of LCC-induced historical albedo changes closer to the -0.15 W/m^2 put forward by Ghimire *et al.*, (2014), who combined the LUHa product with an observational constraint based on satellite data. The fact that Smith *et al.* (2020) found a slightly more negative multi-model mean RF (-0.014 W/m^2) than our best estimate using RFMIP experiments may suggest it, but further analysis of CMIP6 simulations and notably within the Land Use Model Intercomparison Project (LUMIP, Lawrence *et al.*, 2016) are needed before robust conclusions can be drawn. Furthermore, there also exist uncertainties about the HYDE3.1 dataset (Klein Goldewijk *et al.*, 2011) on which the LUHa product is based, as significant differences with the land cover reconstructions from Kaplan *et al.* (2011) and Pongratz *et al.* (2008) have been identified (Schmidt *et al.*, 2012).

The analysis of the biases in the representation of the albedo of trees and crops/grasses in CMIP5 models performed in this study has been focussed on the months of January and July, during which the snow cover fraction is rather correctly represented in CMIP5 models (Thackeray, Fletcher and Derksen, 2015). It could however be repeated for other months and especially in spring and autumn, where misrepresentations in the timing of snow accumulation and melt as well as snow aging processes, LAI parameterisations and the ensuing vegetation masking effect on snow have been identified over the boreal latitudes (Thackeray, Fletcher and Derksen, 2014, 2015; Wang *et al.*, 2016).

Deleted: It illustrates the various ways the analysed CMIP5 models interpreted the land use transition maps delivered by the

Deleted: Hurtt *et al.*, 2011).

Deleted: land-cover changes, a

Deleted: among

Formatted: Font color: Text 1

Deleted: which

Formatted: Font color: Text 1

Formatted: Font color: Text 1

Deleted: land-cover changes

Field Code Changed

Formatted: French

Formatted: French

Formatted: Font color: Text 1

Deleted: Nevertheless, a common dataset for land cover is still subject to uncertainties in land cover reconstructions, as Schmidt *et al.* (2012) have pointed at significant differences between those

Deleted: Kaplan *et al.* (2011),

Deleted: Pongratz *et al.* (2008) and the HYDE3.1 dataset on which the LUHa product is based (Klein Goldewijk *et al.*, 2011)

Deleted: A few more limitations need to be kept in mind when interpreting the findings presented in this study. For example, the albedo sensitivity to deforestation was stronger in pre-industrial times, when the background climate was colder and snow extended over larger land areas. Although Boisier *et al.* (2012) and de Noblet-Ducoudré *et al.* (2012) have shown that changes in background climate have had a very limited impact on the regionally averaged LCC-induced albedo changes, re-calculating the observation-constrained RF with pre-industrial albedo sensitivities may give more negative values, especially locally over high-latitude regions. This interplay between different climate drivers can however not be captured with the RF framework, which assumes that their effects are additive (Myhre *et al.*, 2013). It is also of limited use to investigate

Deleted: 18¶

When interpreting the findings presented in this study, it also needs to be kept in mind that the RF framework is not sufficient to capture the impact of land-cover changes on other climate variables than albedo, as it cannot represent their non-radiative biogeophysical effects (i.e., that solely affect the partitioning between latent and sensible heat fluxes, see e.g. Davin, de Noblet-Ducoudré and Friedlingstein, 2007). Moreover, in this study we have focused our attention on local LCC-induced albedo changes, although those also led to an important remote cooling in global-scale deforestation experiments conducted with the IPSL model (Davin and de Noblet-Ducoudré, 2010).

In conclusion, we demonstrated the suitability of a new methodology to extract the albedo of trees and crops/grasses in ESM simulations that only provide mean albedo values over grid cells containing a diversity of land cover types. After applying it to historical CMIP5 simulations, we identified significant model biases in the representation of the albedo of both trees and crops/grasses, as well as the albedo change arising from a transition between these two land cover types. Additionally, we reconstructed local albedo modifications due to historical LCC. Since these reconstructions are affected by model biases, we used the observed albedo response to transitions between trees and crops/grasses to derive an observation-constrained RF of historical LCC in CMIP5 models. Compared to IPCC AR5 estimates, our results point to a slightly less strong global mean RF, with some remaining uncertainty due to the various magnitudes of LCC implemented in the analysed models. With the release of new ESM simulations within CMIP6 (Eyring *et al.*, 2016), new opportunities arise to assess whether the biases identified in this study have been corrected in the latest generation of ESMs. In that respect, the reconstruction methodology developed for this analysis and which has been implemented as a diagnostic in the ESMValTool v2.0 (Eyring *et al.*, 2020) should allow for a more straightforward model evaluation. Additionally, the new approach to harmonise the forcing from historical LCC in CMIP6 may enable to identify a refined estimate of their RF. We advance that combining recently released observational evidence and model results as proposed in this study will be useful in this context, in order to further reduce uncertainties on the climate impact of historical LCC on both global and local scales.

References

Alkama, R. and Cescatti, A. (2016) 'Biophysical climate impacts of recent changes in global forest cover', *Science*, 351(6273).

Andrews, T. *et al.* (2017) 'Effective radiative forcing from historical land use change', *Climate Dynamics*. Springer Verlag, 48(11–12), pp. 3489–3505. doi: 10.1007/s00382-016-3280-7.

Arino, O. *et al.* (2012) *Global Land Cover Map for 2009 (GlobCover 2009)*, *European Space Agency (ESA) & Université catholique de Louvain (UCL)*. doi: 10.1594/PANGAEA.787668.

Baldocchi, D. *et al.* (2001) *FLUXNET: A New Tool to Study the Temporal and Spatial Variability of Ecosystem-Scale Carbon Dioxide, Water Vapor, and Energy Flux Densities*, *Bulletin of the American Meteorological Society*. doi: 10.1175/1520-0477(2001)082<2415:FANTTS>2.3.CO;2.

Betts, R. A. *et al.* (2007) 'Biogeophysical effects of land use on climate: Model simulations of radiative forcing and large-

Deleted:).

Deleted: at

Formatted: Font color: Text 1

Deleted: In that respect, the reconstruction methodology developed for this analysis and which has been implemented as a diagnostic in the ESMValTool v2.0 (Eyring *et al.*, 2019)

Formatted: Font color: Text 1

Deleted: suggest

Deleted: 19¶

scale temperature change', *Agricultural and Forest Meteorology*, 142(2–4), pp. 216–233. doi: 10.1016/j.agrformet.2006.08.021.

Boisier, J. P. *et al.* (2012) 'Attributing the impacts of land-cover changes in temperate regions on surface temperature and heat fluxes to specific causes : Results from the first LUCID set of simulations', 117, pp. 1–16. doi: 10.1029/2011JD017106.

Boisier, J. P. *et al.* (2013) 'Inferring past land use-induced changes in surface albedo from satellite observations : a useful tool to evaluate model simulations'. doi: 10.5194/bg-10-1501-2013.

Bontemps, S. *et al.* (2011) *GLOBCOVER 2009 Products Description and Validation Report*, *ESA Bulletin*. doi: 10013/epic.39884.d016.

Bright, R. M. and O'halloran, T. L. (2019) 'Developing a monthly radiative kernel for surface albedo change from satellite climatologies of Earth's shortwave radiation budget: CACK v1.0', *Geosci. Model Dev*, 12, pp. 3975–3990. doi: 10.5194/gmd-12-3975-2019.

Brovkin, V. *et al.* (2013) 'Effect of Anthropogenic Land-Use and Land-Cover Changes on Climate and Land Carbon Storage in CMIP5 Projections for the Twenty-First Century', *Journal of Climate*. American Meteorological Society, 26(18), pp. 6859–6881. doi: 10.1175/JCLI-D-12-00623.1.

CERES Science Team (2018) *ASDC | CERES_EBAF-Surface_Edition4.0*. Available at: https://asdc.larc.nasa.gov/project/CERES/CERES_EBAF-Surface_Edition4.0 (Accessed: 6 July 2020).

Cescatti, A. *et al.* (2012) 'Intercomparison of MODIS albedo retrievals and in situ measurements across the global FLUXNET network', *Remote Sensing of Environment*, 121, pp. 323–334. doi: 10.1016/j.rse.2012.02.019.

Chen, L. and Dirmeyer, P. A. (2019) 'Global observed and modelled impacts of irrigation on surface temperature', *International Journal of Climatology*, 39(5), pp. 2587–2600. doi: 10.1002/joc.5973.

Davies-Barnard, T. *et al.* (2014) 'Climatic Impacts of Land-Use Change due to Crop Yield Increases and a Universal Carbon Tax from a Scenario Model', *Journal of Climate*, 27, pp. 1413–1424. doi: 10.1175/JCLI-D-13.

Davin, E. L. and de Noblet-Ducoudré, N. (2010) 'Climatic Impact of Global-Scale Deforestation : Radiative versus Nonradiative Processes', pp. 97–112. doi: 10.1175/2009JCLI3102.1.

Davin, E. L., de Noblet-Ducoudré, N. and Friedlingstein, P. (2007) 'Impact of land cover change on surface climate: Relevance of the radiative forcing concept', *Geophysical Research Letters*, 34(13). doi: 10.1029/2007GL029678.

Duveiller, G. *et al.* (2018) 'Biophysics and vegetation cover change: A process-based evaluation framework for confronting land surface models with satellite observations', *Earth System Science Data*, 10(3), pp. 1265–1279. doi: 10.5194/essd-10-1265-2018.

Duveiller, G. *et al.* (2020) 'Local biophysical effects of land use and land cover change: towards an assessment tool for policy makers', *Land Use Policy*, 91, p. 104382. doi: 10.1016/j.landusepol.2019.104382.

Duveiller, G., Hooker, J. and Cescatti, A. (2018a) 'A dataset mapping the potential biophysical effects of vegetation cover change', *Scientific Data*. Nature Publishing Groups, 5. doi: 10.1038/sdata.2018.14.

Duveiller, G., Hooker, J. and Cescatti, A. (2018b) 'The mark of vegetation change on Earth's surface energy balance', *Nature*

Formatted: English (US)

Formatted: English (US)

Deleted: Cherubini, F., Bright, R. M. and Strømman, A. H. (2012) 'Site-specific global warming potentials of biogenic CO2 for bioenergy: contributions from carbon fluxes and albedo dynamics', *Environ. Res. Lett*, 7, p. 45902. doi: 10.1088/1748-9326/7/4/045902.¶

Deleted: Davin, Edouard L., de Noblet-Ducoudré, N. and Friedlingstein, P. (2007) 'Impact of land cover change on surface climate: Relevance of the radiative forcing concept', *Geophysical Research Letters*, 34(13). doi: 10.1029/2007GL029678.¶

Deleted:), p. n/a-n/a.

Deleted: 20¶

Communications. Springer US, 9(1). doi: 10.1038/s41467-017-02810-8.

Efron, B. (1982) '6. The Infinitesimal Jackknife, the Delta Method and the Influence Function', in *The Jackknife, the Bootstrap and Other Resampling Plans*. Society for Industrial and Applied Mathematics, pp. 37–47. doi: 10.1137/1.9781611970319.ch6.

Eyring, V. *et al.* (2016) 'Overview of the Coupled Model Intercomparison Project Phase 6 (CMIP6) experimental design and organization', *Geoscientific Model Development*, 9(5), pp. 1937–1958. doi: 10.5194/gmd-9-1937-2016.

Eyring, V. *et al.* (2020) 'Earth System Model Evaluation Tool (ESMValTool) v2.0–an extended set of large-scale diagnostics for quasi-operational and comprehensive evaluation of Earth system models in CMIP', *NCAS Computational Modelling Services*, 13, pp. 3383–3438. doi: 10.5194/gmd-13-3383-2020.

Foley, J. A. *et al.* (2005) 'Global consequences of land use', *Science*, pp. 570–574. doi: 10.1126/science.1111772.

Ghimire, B. *et al.* (2014) 'Global albedo change and radiative cooling from anthropogenic land cover change, 1700 to 2005 based on MODIS, land use harmonization, radiative kernels, and reanalysis', *Geophysical Research Letters*. Blackwell Publishing Ltd, 41(24), pp. 9087–9096. doi: 10.1002/2014GL061671.

Harris, I. *et al.* (2014) 'Updated high-resolution grids of monthly climatic observations - the CRU TS3.10 Dataset', *International Journal of Climatology*, 34(3), pp. 623–642. doi: 10.1002/joc.3711.

Hurtt, G. C. *et al.* (2011) 'Harmonization of land-use scenarios for the period 1500-2100: 600 years of global gridded annual land-use transitions, wood harvest, and resulting secondary lands', *Climatic Change*, 109, pp. 117–161. doi: 10.1007/s10584-011-0153-2.

Kaplan, J. O. *et al.* (2011) 'Holocene carbon emissions as a result of anthropogenic land cover change', *Holocene*, 21(5), pp. 775–791. doi: 10.1177/0959683610386983.

Klein Goldewijk, K. *et al.* (2011) 'The HYDE 3.1 spatially explicit database of human-induced global land-use change over the past 12,000 years', *Global Ecology and Biogeography*, 20(1), pp. 73–86. doi: 10.1111/j.1466-8238.2010.00587.x.

Kvalevåg, M. M. *et al.* (2010) 'Anthropogenic land cover changes in a GCM with surface albedo changes based on MODIS data', *International Journal of Climatology*, 30(13), pp. 2105–2117. doi: 10.1002/joc.2012.

Lawrence, D. M. *et al.* (2016) 'The Land Use Model Intercomparison Project (LUMIP) contribution to CMIP6: Rationale and experimental design', *Geoscientific Model Development*, 9(9), pp. 2973–2998. doi: 10.5194/gmd-9-2973-2016.

Lawrence, P. J. and Chase, T. N. (2007) 'Representing a new MODIS consistent land surface in the Community Land Model (CLM 3.0)', *Journal of Geophysical Research*, 112(G1), p. G01023. doi: 10.1029/2006JG000168.

Lejeune, Q. *et al.* (2018) 'Historical deforestation locally increased the intensity of hot days in northern mid-latitudes', *Nature Climate Change*. Springer US, 8(5), pp. 386–390. doi: 10.1038/s41558-018-0131-z.

Lejeune, Q., Seneviratne, S. I. and Davin, E. L. (2017) 'Historical land-cover change impacts on climate: Comparative assessment of LUCID and CMIP5 multimodel experiments', *Journal of Climate*, 30(4), pp. 1439–1459. doi: 10.1175/JCLI-D-16-0213.1.

Lenton, T. M. and Vaughan, N. E. (2009) *The radiative forcing potential of different climate geoengineering options*, *Atmos. Chem. Phys*. Available at: www.atmos-chem-phys.net/9/5539/2009/ (Accessed: 6 December 2019).

Deleted: 2019) '

Deleted: .

Deleted: – Extended

Deleted: (November).

Formatted: English (US)

Formatted: English (US)

Formatted: English (US)

Deleted: Lacis, A. A. and Hansen, J. E. (1974) 'A Parameterization for the Absorption of Solar Radiation in the Earth's Atmosphere', *Journal of the Atmospheric Sciences*, 31, pp. 118–133.¶

Deleted: 21¶

Lewis, P. *et al.* (2012) 'The ESA globAlbedo project: Algorithm', *International Geoscience and Remote Sensing Symposium (IGARSS)*, (February 2015), pp. 5745–5748. doi: 10.1109/IGARSS.2012.6352306.

Lewis, X. P. *et al.* (2013) *GlobAlbedo Algorithm Theoretical Basis Document*.

Li, Y. *et al.* (2015) 'Local cooling and warming effects of forests based on satellite observations', *Nature Communications*. Nature Publishing Group, 6, pp. 1–8. doi: 10.1038/ncomms7603.

Mahmood, R. *et al.* (2014) 'Land cover changes and their biogeophysical effects on climate', *International Journal of Climatology*, 34(4), pp. 929–953. doi: 10.1002/joc.3736.

Malyshev, S. *et al.* (2015) 'Contrasting Local versus Regional Effects of Land-Use-Change-Induced Heterogeneity on Historical Climate: Analysis with the GFDL Earth System Model', *Journal of Climate*, 28, pp. 5448–5469. doi: 10.1175/JCLI-D-14-00586.1.

Meier, R. *et al.* (2018) 'Evaluating and improving the Community Land Model's sensitivity to land cover', *Biogeosciences*, 15, pp. 4731–4757. doi: 10.5194/bg-15-4731-2018.

Muller, J.-P. *et al.* (2013) *GlobAlbedo Final Product Validation Report*.

Myhre, G. *et al.* (2013) 'Anthropogenic and Natural Radiative Forcing', in Stocker, T. F. et al. (eds) *Climate Change 2013: The Physical Science Basis. Contribution of Working Group I to the Fifth Assessment Report of the Intergovernmental Panel on Climate Change*. Cambridge, UK and New York, US: Cambridge University Press, p. in press.

Myhre, Gunnar *et al.* (2013) 'Anthropogenic and Natural Radiative Forcing', *Climate Change 2013: The Physical Science Basis. Contribution of Working Group I to the Fifth Assessment Report of the Intergovernmental Panel on Climate Change*, pp. 659–740. doi: 10.1017/ CBO9781107415324.018.

Myhre, G., Kvalevåg, M. M. and Schaaf, C. B. (2005) 'Radiative forcing due to anthropogenic vegetation change based on MODIS surface albedo data', *Geophysical Research Letters*, 32(21), p. L21410. doi: 10.1029/2005GL024004.

de Noblet-Ducoudré, N. *et al.* (2012) 'Determining Robust Impacts of Land-Use-Induced Land Cover Changes on Surface Climate over North America and Eurasia : Results from the First Set of LUCID Experiments'. doi: 10.1175/JCLI-D-11-00338.1.

Oleson, K. W. *et al.* (2013) 'NCAR/TN-503+STR NCAR Technical Note Technical Description of version 4.5 of the Community Land Model (CLM) Coordinating Lead Authors'. Available at: http://library.ucar.edu/research/publish-technote (Accessed: 31 December 2019).

Pitman, A. J. *et al.* (2009) 'Uncertainties in climate responses to past land cover change: First results from the LUCID intercomparison study', *Geophysical Research Letters*, 36(14), pp. 1–6. doi: 10.1029/2009GL039076.

Pongratz, J. *et al.* (2008) 'A reconstruction of global agricultural areas and land cover for the last millennium', *Global Biogeochemical Cycles*, 22(3), p. n/a-n/a. doi: 10.1029/2007GB003153.

Pongratz, J. *et al.* (2009) 'Radiative forcing from anthropogenic land cover change since A.D. 800', *Geophysical Research Letters*, 36(2), p. n/a-n/a. doi: 10.1029/2008GL036394.

Pongratz, J. *et al.* (2010) 'Biogeophysical versus biogeochemical climate response to historical anthropogenic land cover

Formatted: English (US)

Deleted: 22¶

change', *Geophysical Research Letters*, 37(8), pp. 1–5. doi: 10.1029/2010GL043010.
Qu, X. and Hall, A. (2007) 'What Controls the Strength of Snow-Albedo Feedback?' doi: 10.1175/JCLI4186.1.
Ramankutty, N. and Foley, J. A. (1999) 'Estimating historical changes in global land cover: Croplands from 1700 to 1992', *Global Biogeochemical Cycles*, 13(4), pp. 997–1027. doi: 10.1029/1999GB900046.
Schaaf, C. B. *et al.* (2002) 'First operational BRDF, albedo nadir reflectance products from MODIS', *Remote Sensing of Environment*, 83(1–2), pp. 135–148. doi: 10.1016/S0034-4257(02)00091-3.
Schmidt, G. a. *et al.* (2012) 'Climate forcing reconstructions for use in PMIP simulations of the Last Millennium (v1.1)', *Geoscientific Model Development*, 5(1), pp. 185–191. doi: 10.5194/gmd-5-185-2012.
Smith, C. J. *et al.* (2020) 'Effective radiative forcing and adjustments in CMIP6 models', *Atmos. Chem. Phys*, 20, pp. 9591–9618. doi: 10.5194/acp-20-9591-2020.
Soden, B. J. *et al.* (2008) 'Quantifying Climate Feedbacks Using Radiative Kernels'. doi: 10.1175/2007JCLI2110.1.
Taylor, K. E., Stouffer, R. J. and Meehl, G. a. (2012) 'An Overview of CMIP5 and the Experiment Design', *Bulletin of the American Meteorological Society*, 93(4), pp. 485–498. doi: 10.1175/BAMS-D-11-00094.1.
Thackeray, C. W., Fletcher, C. G. and Derksen, C. (2014) 'The influence of canopy snow parameterizations on snow albedo feedback in boreal forest regions', *Journal of Geophysical Research: Atmospheres*. American Geophysical Union (AGU), 119(16), pp. 9810–9821. doi: 10.1002/2014jd021858.
Thackeray, C. W., Fletcher, C. G. and Derksen, C. (2015) 'Quantifying the skill of CMIP5 models in simulating seasonal albedo and snow cover evolution', *Journal of Geophysical Research: Atmospheres*. Wiley-Blackwell, 120(12), pp. 5831–5849. doi: 10.1002/2015JD023325.
Di Vittorio, A. V *et al.* (2014) 'From land use to land cover: restoring the afforestation signal in a coupled integrated assessment-earth system model and the implications for CMIP5 RCP simulations', *Biogeosciences*, 11, pp. 6435–6450. doi: 10.5194/bg-11-6435-2014.
Wang, L. *et al.* (2016) 'Investigating the spread in surface albedo for snow-covered forests in CMIP5 models', *Journal of Geophysical Research: Atmospheres*. Wiley-Blackwell, 121(3), pp. 1104–1119. doi: 10.1002/2015JD023824.
Winckler, J. *et al.* (2019) 'Nonlocal Effects Dominate the Global Mean Surface Temperature Response to the Biogeophysical Effects of Deforestation', *Geophysical Research Letters*, 46(2), pp. 745–755. doi: 10.1029/2018GL080211.
Winckler, J., Reick, C. H. and Pongratz, J. (2017) 'Robust identification of local biogeophysical effects of land-cover change in a global climate model', *Journal of Climate*, 30(3), pp. 1159–1176. doi: 10.1175/JCLI-D-16-0067.1.

Formatted: English (US)

Formatted: English (US)

Formatted: English (US)

Formatted: Font: 9 pt, Bold

Deleted: 23¶

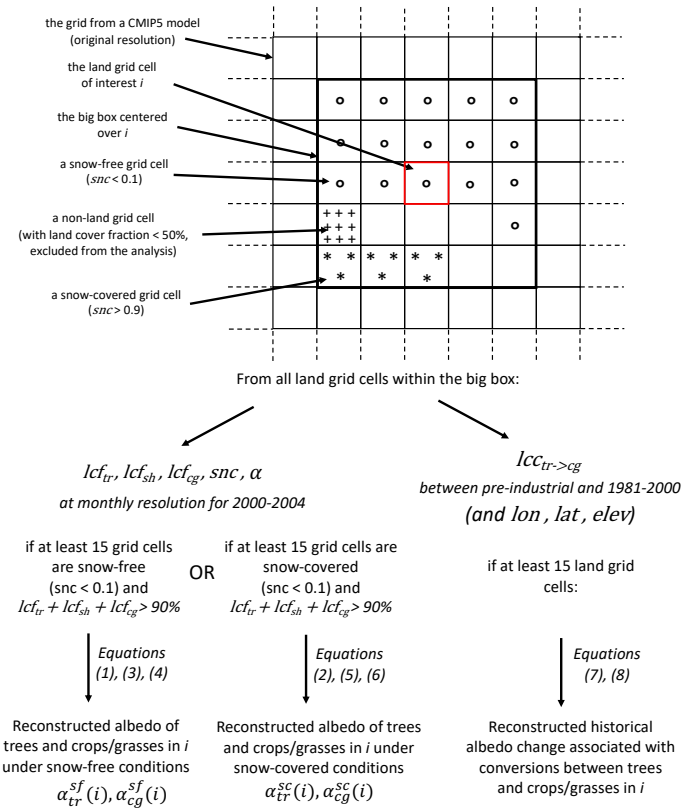

1: Description of the two employed reconstruction methodologies. *snc* stands for snow cover fraction, *α* for albedo, *lcf* for land cover fraction, *lcc* for land cover conversion, the suffixes *tr*, *sh* and *cg* for trees, shrubs and crops/grasses, respectively, *lon* for longitude, *lat* for latitude, and *elev* for elevation.

Moved (insertion) [2]

Deleted: Figure RMSE ... [111]

Formatted: Font: 9 pt, Bold

Deleted: 24¶

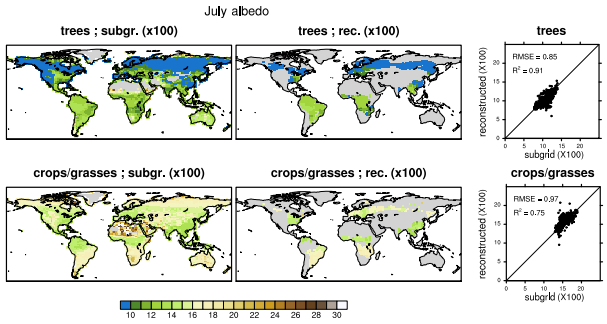

Figure 2: Subgrid (left) and reconstructed (middle) estimates of the present-day (2002-2010) albedo of trees (upper row) and crops/grasses (lower row) in the CLM4.5 simulations, for the month of July. The scatter plots (right) indicate the relationship between reconstructed (y-axis) and subgrid estimates (x-axis), with each dot indicating the results of a grid cell for which both methods could be applied. Note that albedo values have been multiplied by 100 to facilitate readability.

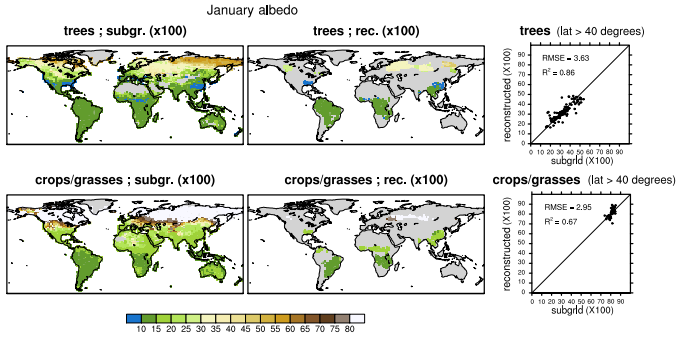

Figure 3: Same as Figure 2, but for the month of January. The scatter plots in this case only display the results for the grid cells north of 40° (i.e., over areas considered as snow-covered). Note that the scale is different.

Deleted: right

Deleted: Note that absolute differences

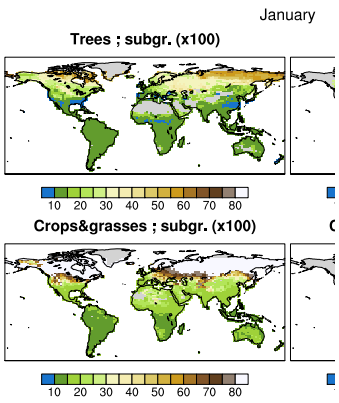

Deleted:

Deleted: 2

Deleted: 1

Deleted: 25¶

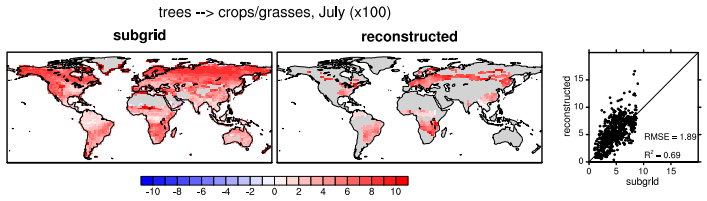

Figure 4: Subgrid (left) and reconstructed (right) estimates of the present-day (2002-2010) potential albedo change associated to a transition from trees to crops/grasses in the CLM4.5 simulations, for the month of July. Note that absolute differences have been multiplied by 100 to facilitate reading.

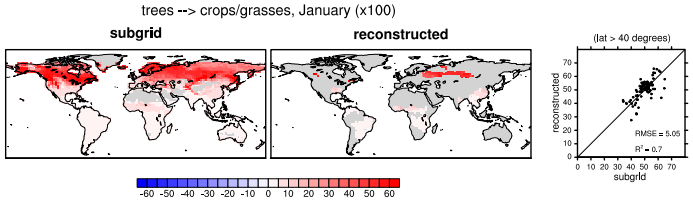

Figure 5: Same as Figure 4, but for the month of January. The scatter plots in this case only display the results for the grid cells north of 40° (i.e., over areas considered as snow-covered). Note that the scale is different.

July

deforestation ; subgr. (x100)

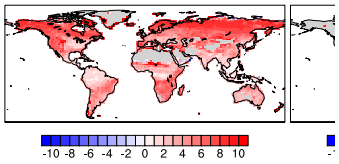

Deleted:

Deleted: 3

January

deforestation ; subgr. (x100)

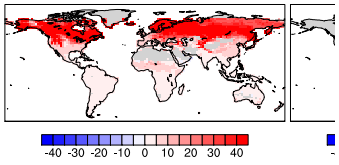

Deleted:

Deleted: 4

Deleted: 3

Deleted: 26¶

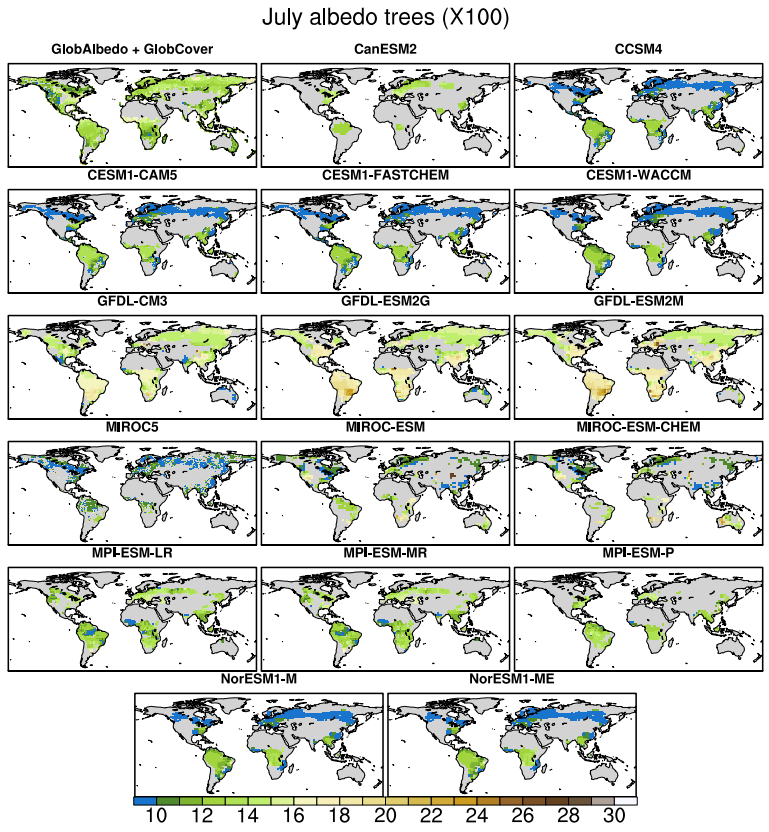

375

Figure 6: Present-day July albedo of trees retrieved from the combination of the observational data GlobAlbedo and GlobCover (top-left corner) and in the analysed CMIP5 models. Note that the albedo values have been multiplied by 100 to facilitate readability.

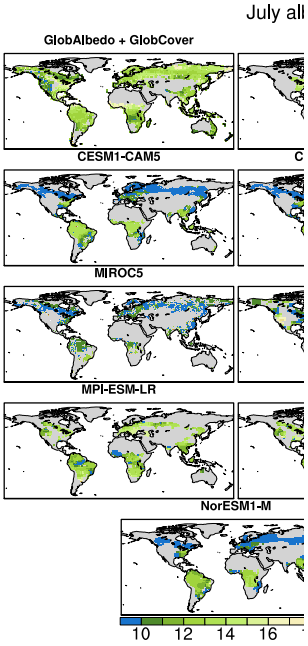

Deleted:

Deleted: 5:

Deleted: 27¶

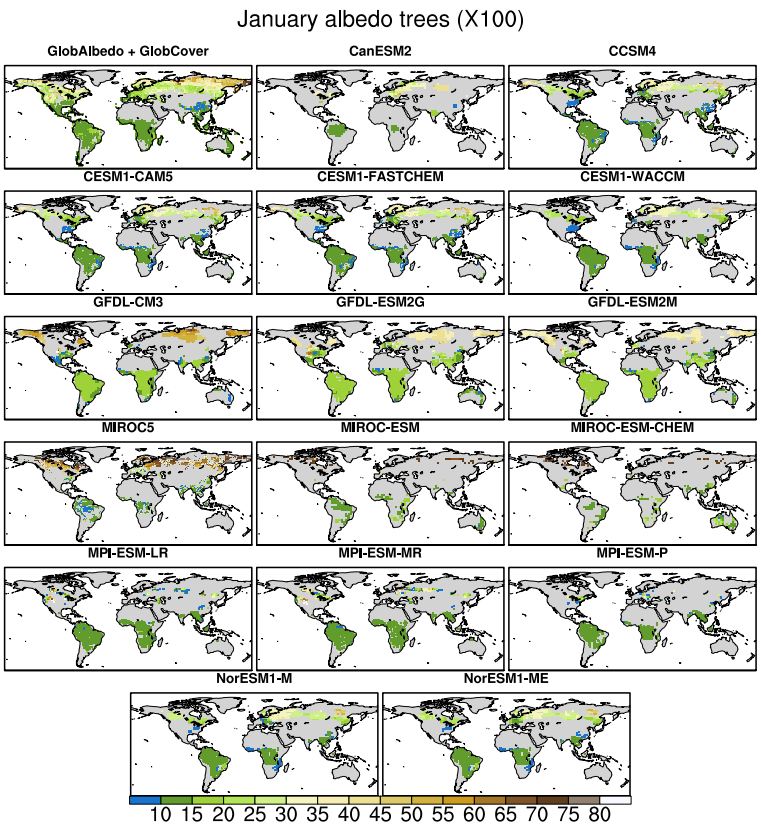

Figure 7: Same as Figure 6, but for the month of January. Note that the scale is different.

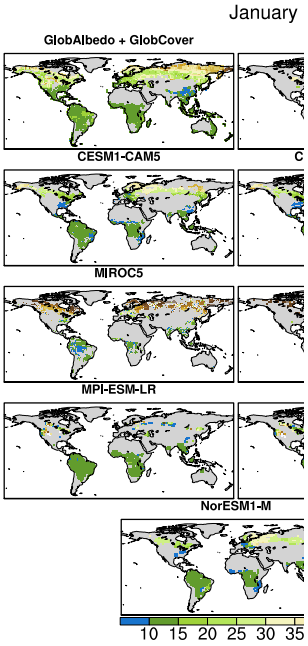

Deleted:

Deleted: 6…: Same as Figure 5 ... [112]

Deleted: 28¶

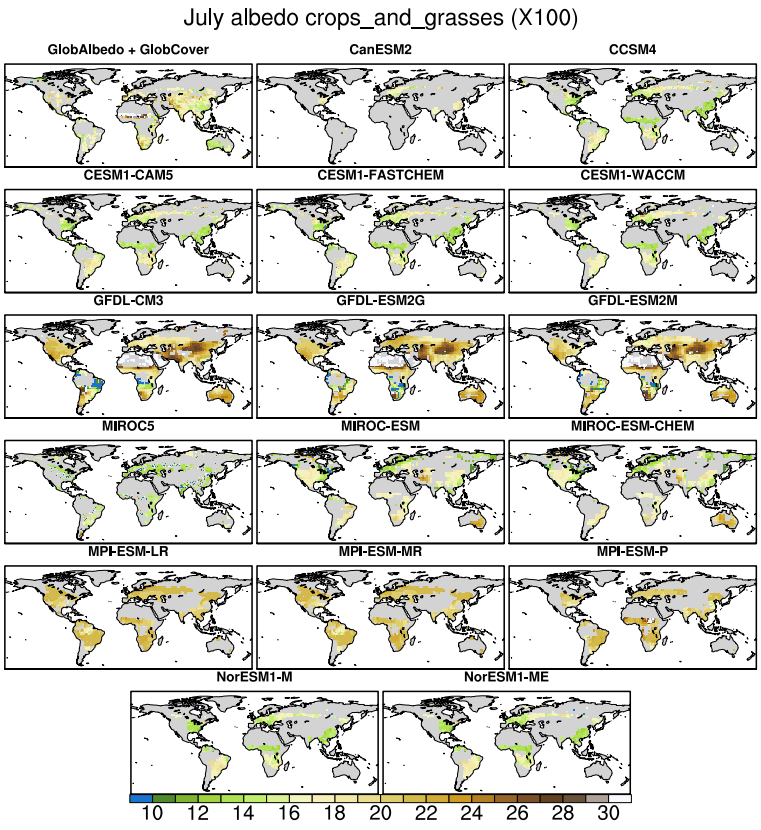

Figure 8: Present-day July albedo of crops/grasses according to the combined observational data GlobAlbedo and GlobCover (top-left corner) and in the analysed CMIP5 models. Note that the albedo values have been multiplied by 100 to facilitate readability.

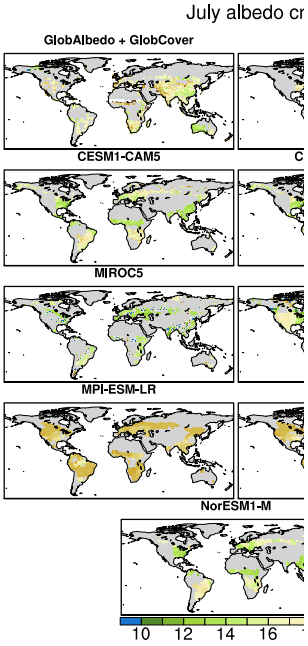

Deleted:

Deleted: 7:

Deleted: 29¶

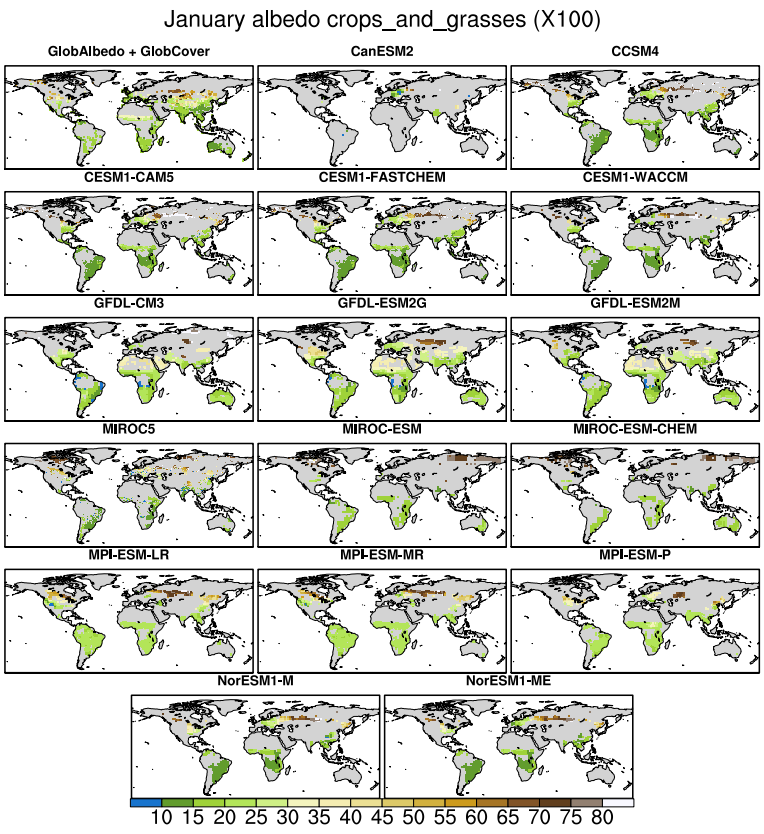

Figure 9: Same as Figure 8, but for the month of January. Note that the scale is different.

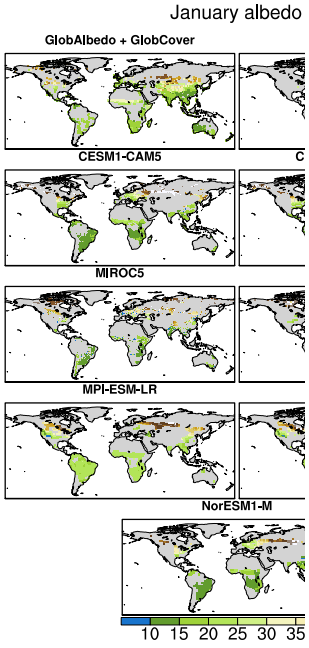

Deleted:

Deleted: 8…: Same as Figure 7 ... [113]

Deleted: 30¶

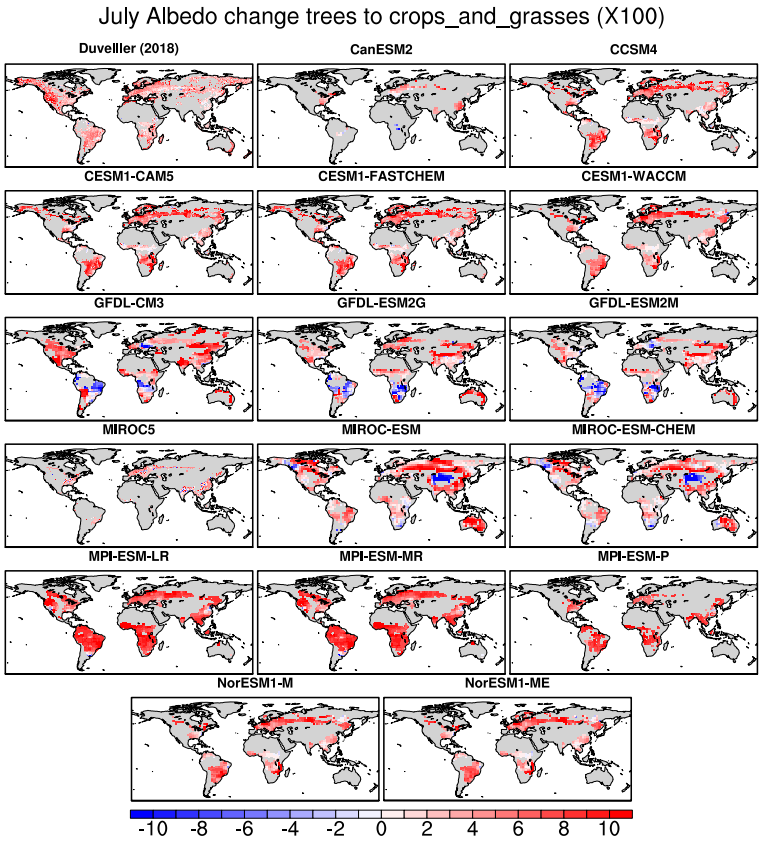

Figure 10: Potential present-day July albedo change associated to a transition from trees to crops/grasses according to the observational dataset of Duveiller, Hooker and Cescatti (2018a)**, top-left corner) and in the analysed CMIP5 models. Note that the absolute differences have been multiplied by 100 to facilitate readability.**

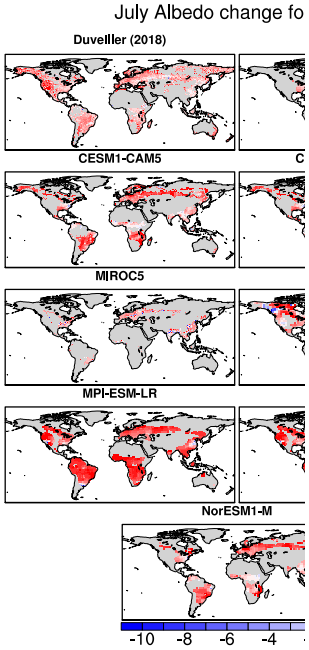

Deleted: ... [114]

Deleted: 31¶

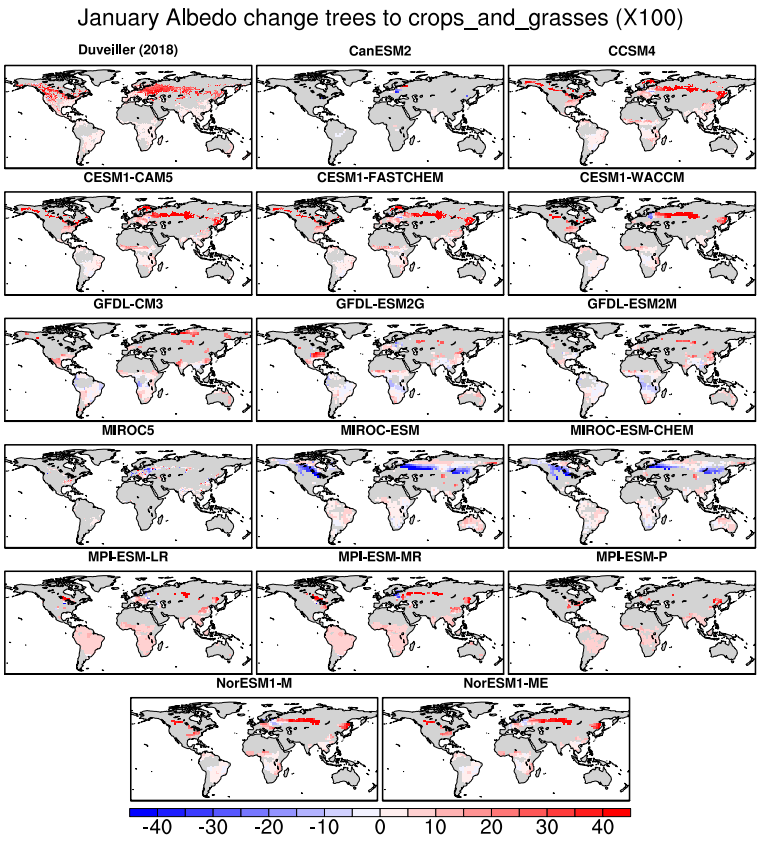

Figure 11: Same as Figure 10, but for January. Note that the scale is different.

Deleted: 10

Deleted: 9

Deleted: 32¶

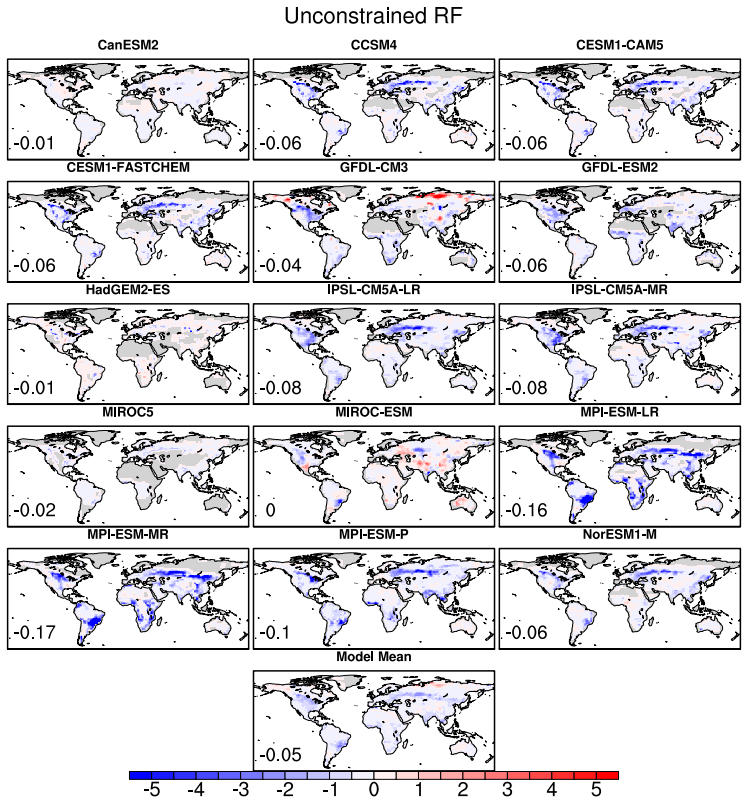

Figure 12: Radiative Forcing from historical conversions between trees and crops/grasses (from the pre-industrial to the 1981-2000 period) in the analysed CMIP5 models (in W/m^2), obtained by applying the reconstruction method (see the description of the methodology in Section 2.4). The numbers in the bottom-left corner of each map indicate the global mean Radiative Forcing. For the computation of the Model Mean, if several CMIP5 models contain the same Land Surface Model they were attributed a lower weight so that the sum of their weights equal 1.

Deleted:

Deleted: 11…2: Radiative Forcing from historical deforestation…onversions between trees and crops/grasses (from the pre-industrial to the 1981-2000 period) in the analysed CMIP5 models (in W/m^2), obtained by applying the reconstruction method….(see the description of the methodology in Section 2.4). The numbers in the bottom-left corner of each map indicate the global mean Radiative Forcing from historical deforestation.¶ … [115]

Moved up [2]: ¶
Figure

Deleted: 12: Observation-constrained Radiative Forcing from historical deforestation in the analysed CMIP5 models (in W/m^2).

Moved down [3]: The numbers in the bottom-left corner of each map indicate the global mean Radiative Forcing.

Deleted: To compute… For the computation of the Model Mean, if several CMIP5 models contain the same Land Surface Model they were attributed a lower weight so that the sum of these…heir weights equal 1. … [116]

Deleted: 33¶

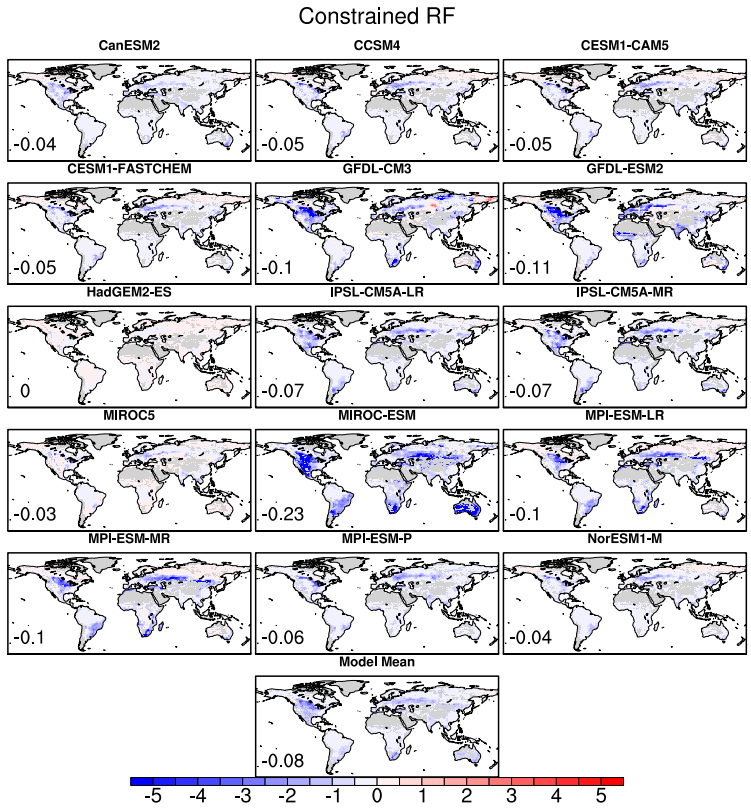

Figure 13: Observation-constrained Radiative Forcing from historical conversions between trees and crops/grasses (from the pre-industrial to the 1981-2000 period) in the analysed CMIP5 models (in W/m^2). The numbers in the bottom-left corner of each map indicate the global mean Radiative Forcing.

Moved (insertion) [3]

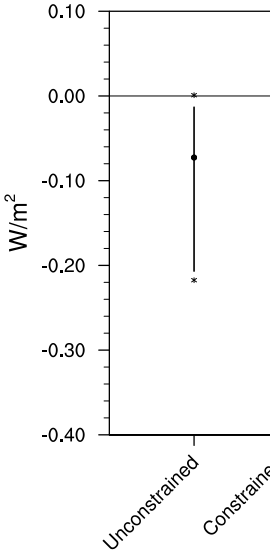

Deleted:

Deleted: 34¶

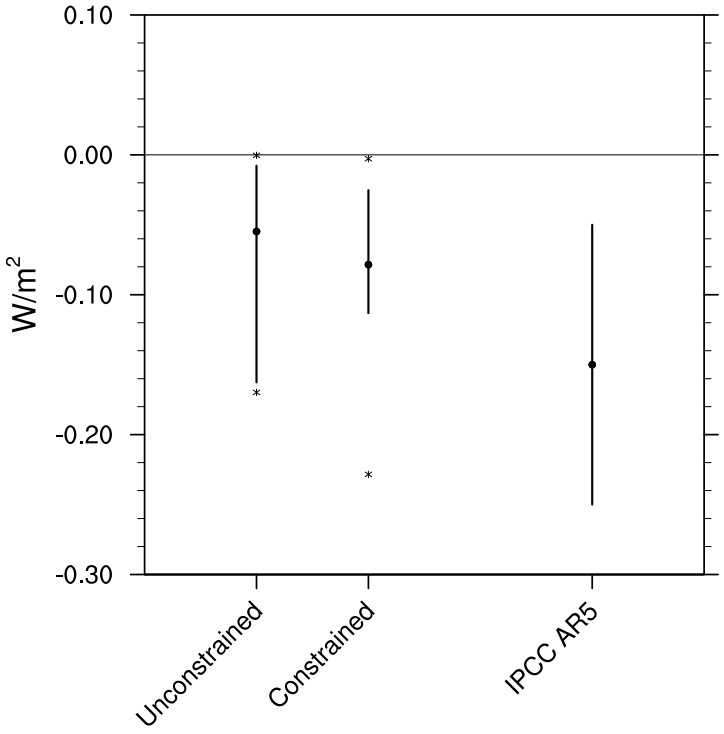

Figure 14: Spread in the unconstrained (left bar) and observation-constrained (middle bar) estimates of the global Radiative Forcing from historical conversions between trees and crops/grasses (from the pre-industrial to the 1981-2000 periods), for the CMIP5 models shown in Figures 11 and 12 (in W/m^2), as well as the IPCC AR5 estimate of the global Radiative Forcing from historical land-use changes (mean estimate and spread as in Myhre *et al.*, 2013). The dots on the left and middle bars show the Model Mean results for the unconstrained and observation-constrained estimates, respectively, the asterisks mark the lowest and highest values for each category, while the lengths of the bars indicate the spread between the remaining values (i.e., excluding the highest and lowest ones).

Deleted: 13
Deleted: deforestation
Deleted: (Myhre *et al.*, 2013)).
Deleted: model mean
Deleted: value
Deleted: first and ninth deciles.
Formatted: Font: 9 pt, Bold
Formatted: Normal

Deleted: 35¶

Page 1: [1] Style Definition **9/1/20 1:43:00 AM**

Comment Text: Font: (Default) Times New Roman, Don't hyphenate

Page 1: [2] Style Definition **9/1/20 1:43:00 AM**

Footer: Suppress line numbers, Don't hyphenate

Page 7: [3] Formatted **9/1/20 1:42:00 AM**

Font: Times New Roman

Page 7: [4] Formatted **9/1/20 1:42:00 AM**

Font: Times New Roman

Page 7: [5] Formatted **9/1/20 1:42:00 AM**

Font: Times New Roman

Page 7: [6] Formatted **9/1/20 1:42:00 AM**

Font: Times New Roman

Page 7: [7] Formatted **9/1/20 1:42:00 AM**

Font: Times New Roman

Page 7: [8] Formatted **9/1/20 1:42:00 AM**

Font: Times New Roman

Page 7: [9] Formatted **9/1/20 1:42:00 AM**

Font: Times New Roman

Page 7: [9] Formatted **9/1/20 1:42:00 AM**

Font: Times New Roman

Page 7: [10] Formatted **9/1/20 1:42:00 AM**

Font: Times New Roman

Page 7: [11] Formatted **9/1/20 1:42:00 AM**

Font: Times New Roman

Page 7: [12] Formatted **9/1/20 1:42:00 AM**

Font: Times New Roman

Page 7: [13] Deleted **9/1/20 1:43:00 AM**

Page 7: [14] Formatted **9/1/20 1:42:00 AM**

Font: Times New Roman

Page 7: [15] Formatted **9/1/20 1:42:00 AM**

Page 7: [17] Deleted **9/1/20 1:43:00 AM**

Page 7: [18] Formatted **9/1/20 1:42:00 AM**

Font: Times New Roman

Page 7: [18] Formatted **9/1/20 1:42:00 AM**

Font: Times New Roman

Page 7: [19] Formatted **9/1/20 1:42:00 AM**

Font: Times New Roman

Page 7: [20] Deleted **9/1/20 1:43:00 AM**

Page 7: [21] Formatted **9/1/20 1:42:00 AM**

Font: Times New Roman

Page 7: [22] Formatted **9/1/20 1:42:00 AM**

Font: Times New Roman

Page 7: [23] Formatted **9/1/20 1:42:00 AM**

Font: Times New Roman

Page 7: [24] Deleted **9/1/20 1:43:00 AM**

Page 7: [25] Formatted **9/1/20 1:42:00 AM**

Font: Times New Roman

Page 7: [26] Formatted **9/1/20 1:42:00 AM**

Font: Times New Roman

Page 7: [27] Formatted **9/1/20 1:42:00 AM**

Font: Times New Roman

Page 7: [28] Formatted **9/1/20 1:42:00 AM**

Font: Times New Roman

Page 7: [29] Formatted **9/1/20 1:42:00 AM**

Font: Times New Roman

Page 7: [30] Formatted **9/1/20 1:42:00 AM**

Font: Times New Roman

Page 7: [31] Formatted **9/1/20 1:42:00 AM**

Page 7: [34] Formatted **9/1/20 1:42:00 AM**

Font: Times New Roman

Page 7: [35] Formatted **9/1/20 1:42:00 AM**

Font: Times New Roman

Page 7: [36] Formatted **9/1/20 1:42:00 AM**

Font: Times New Roman

Page 7: [37] Formatted **9/1/20 1:42:00 AM**

Font: Times New Roman

Page 7: [38] Formatted **9/1/20 1:42:00 AM**

Font: Times New Roman

Page 7: [39] Formatted **9/1/20 1:42:00 AM**

Font: Times New Roman

Page 7: [40] Formatted **9/1/20 1:42:00 AM**

Font: Times New Roman

Page 7: [41] Formatted **9/1/20 1:42:00 AM**

Font: Times New Roman

Page 7: [42] Formatted **9/1/20 1:42:00 AM**

Font: Times New Roman

Page 7: [43] Formatted **9/1/20 1:42:00 AM**

Font: Times New Roman

Page 7: [44] Formatted **9/1/20 1:42:00 AM**

Font: Times New Roman

Page 7: [45] Formatted **9/1/20 1:42:00 AM**

Font: Times New Roman

Page 7: [46] Formatted **9/1/20 1:42:00 AM**

Font: Times New Roman

Page 7: [47] Formatted **9/1/20 1:42:00 AM**

Font: Times New Roman

Page 7: [48] Formatted **9/1/20 1:42:00 AM**

Font: Times New Roman

Page 7: [49] Formatted **9/1/20 1:42:00 AM**

Page 7: [52] Formatted **9/1/20 1:42:00 AM**

Font: Times New Roman

Page 7: [53] Formatted **9/1/20 1:42:00 AM**

Font: Times New Roman

Page 7: [54] Formatted **9/1/20 1:42:00 AM**

Font: Times New Roman

Page 7: [55] Formatted **9/1/20 1:42:00 AM**

Font: Times New Roman

Page 7: [56] Formatted **9/1/20 1:42:00 AM**

Font: Times New Roman

Page 7: [57] Formatted **9/1/20 1:42:00 AM**

Font: Times New Roman

Page 7: [58] Formatted **9/1/20 1:42:00 AM**

Font: Times New Roman

Page 7: [58] Formatted **9/1/20 1:42:00 AM**

Font: Times New Roman

Page 7: [59] Formatted **9/1/20 1:42:00 AM**

Font: Times New Roman

Page 7: [60] Formatted **9/1/20 1:42:00 AM**

Font: Times New Roman

Page 8: [61] Formatted **9/1/20 1:42:00 AM**

Font: Times New Roman

Page 8: [62] Formatted **9/1/20 1:42:00 AM**

Font: Times New Roman

Page 8: [63] Formatted **9/1/20 1:42:00 AM**

Font: Times New Roman

Page 8: [64] Formatted **9/1/20 1:42:00 AM**

Font: Times New Roman

Page 8: [65] Formatted **9/1/20 1:42:00 AM**

Font: Times New Roman

Page 8: [69] Formatted **9/1/20 1:42:00 AM**

Font: Times New Roman

Page 8: [69] Formatted **9/1/20 1:42:00 AM**

Font: Times New Roman

Page 8: [70] Formatted **9/1/20 1:42:00 AM**

Font: Times New Roman

Page 8: [71] Formatted **9/1/20 1:42:00 AM**

Font: Times New Roman

Page 8: [72] Formatted **9/1/20 1:42:00 AM**

Font: Times New Roman

Page 8: [73] Formatted **9/1/20 1:42:00 AM**

Font: Times New Roman

Page 8: [73] Formatted **9/1/20 1:42:00 AM**

Font: Times New Roman

Page 8: [74] Formatted **9/1/20 1:42:00 AM**

Font: Times New Roman

Page 8: [75] Formatted **9/1/20 1:42:00 AM**

Font: Times New Roman

Page 8: [76] Deleted **9/1/20 1:43:00 AM**

Page 8: [77] Formatted **9/1/20 1:42:00 AM**

Font: Times New Roman

Page 8: [78] Deleted **9/1/20 1:43:00 AM**

Page 8: [79] Formatted **9/1/20 1:42:00 AM**

Font: Times New Roman

Page 8: [80] Formatted **9/1/20 1:42:00 AM**

Font: Times New Roman

Page 8: [81] Deleted **9/1/20 1:43:00 AM**

Page 8: [85] Formatted **9/1/20 1:42:00 AM**

Outline numbered + Level: 3 + Numbering Style: 1, 2, 3, … + Start at: 1 + Alignment: Left + Aligned at: 0 cm + Indent at: 1,27 cm

Page 8: [86] Formatted **9/1/20 1:42:00 AM**

Font: Times New Roman

Page 8: [86] Formatted **9/1/20 1:42:00 AM**

Font: Times New Roman

Page 8: [87] Formatted **9/1/20 1:42:00 AM**

Font: Times New Roman

Page 8: [87] Formatted **9/1/20 1:42:00 AM**

Font: Times New Roman

Page 8: [88] Formatted **9/1/20 1:42:00 AM**

Font: Times New Roman

Page 8: [89] Formatted **9/1/20 1:42:00 AM**

Font: Times New Roman

Page 8: [90] Formatted **9/1/20 1:42:00 AM**

Font: Times New Roman

Page 8: [91] Formatted **9/1/20 1:42:00 AM**

Font: Times New Roman

Page 8: [92] Formatted **9/1/20 1:42:00 AM**

Font: Times New Roman

Page 8: [93] Formatted **9/1/20 1:42:00 AM**

Font: Times New Roman

Page 8: [94] Formatted **9/1/20 1:42:00 AM**

Font: Times New Roman

Page 8: [94] Formatted **9/1/20 1:42:00 AM**

Font: Times New Roman

Page 8: [95] Deleted **9/1/20 1:43:00 AM**

Page 8: [95] Deleted **9/1/20 1:43:00 AM**

Page 8: [95] Deleted 9/1/20 1:43:00 AM

Page 8: [96] Formatted 9/1/20 1:42:00 AM

Font: Times New Roman

Page 8: [97] Formatted 9/1/20 1:42:00 AM

Font: Times New Roman

Page 8: [98] Formatted 9/1/20 1:42:00 AM

Font: Times New Roman

Page 8: [99] Formatted 9/1/20 1:42:00 AM

Font: Times New Roman

Page 8: [100] Formatted 9/1/20 1:42:00 AM

Font: Times New Roman

Page 8: [101] Formatted 9/1/20 1:42:00 AM

Font: Times New Roman

Page 8: [102] Formatted 9/1/20 1:42:00 AM

Font: Times New Roman

Page 8: [103] Formatted 9/1/20 1:42:00 AM

Font: Times New Roman

Page 8: [104] Formatted 9/1/20 1:42:00 AM

Font: Times New Roman, English (UK)

Page 8: [105] Deleted 9/1/20 1:43:00 AM

Page 9: [106] Formatted 9/1/20 1:42:00 AM

Outline numbered + Level: 2 + Numbering Style: 1, 2, 3, … + Start at: 1 + Alignment: Left + Aligned at: 0 cm + Indent at: 0,74 cm

Page 9: [107] Deleted 9/1/20 1:43:00 AM

Page 10: [108] Formatted 9/1/20 1:42:00 AM

Outline numbered + Level: 1 + Numbering Style: 1, 2, 3, … + Start at: 1 + Alignment: Left + Aligned at: 0 cm + Indent at: 0,63 cm

Page 10: [109] Formatted 9/1/20 1:42:00 AM

Outline numbered + Level: 2 + Numbering Style: 1, 2, 3, … + Start at: 1 + Alignment: Left + Aligned at: 0 cm + Indent at: 0,74 cm

Page 28: [112] Deleted 9/1/20 1:43:00 AM

Page 30: [113] Deleted 9/1/20 1:43:00 AM

Page 30: [113] Deleted 9/1/20 1:43:00 AM

Page 31: [114] Deleted 9/1/20 1:43:00 AM

Page 33: [115] Deleted 9/1/20 1:43:00 AM

Page 33: [115] Deleted 9/1/20 1:43:00 AM

Page 33: [115] Deleted 9/1/20 1:43:00 AM

Page 33: [115] Deleted 9/1/20 1:43:00 AM

Page 33: [116] Deleted 9/1/20 1:43:00 AM

Page 33: [116] Deleted 9/1/20 1:43:00 AM

Page 33: [116] Deleted 9/1/20 1:43:00 AM